Penerbit Akademia Baru

Journal of Advanced Research Design

Journal homepage:
https://akademiabaru.com/submit/index.php/ard
ISSN: 2289-7984

Comprehensive Review on Sensitivity Determination in Fiber Bragg Grating Accelerometer

Nazir Abbas[1], Mohd Firdaus Hassan[1,*]

[1] Faculty of Mechanical and Automotive Engineering Technology, Universiti Malaysia Pahang Al-Sultan Abdullah, 26600 Pekan, Pahang, Malaysia

ARTICLE INFO

Article history:
Received 13 January 2025
Received in revised form 7 February 2025
Accepted 7 April 2025
Available online 30 April 2025

Keywords:
Cantilever FBG accelerometer; sensitivity measurement; frequency-dependent sensitivity; dynamic measurement; machine learning

ABSTRACT

Achieving accurate sensitivity measurements in Fibre Bragg Grating (FBG) sensors is crucial for their reliable application across various fields. This review paper delves into the sensitivity characteristics of FBG sensors, emphasizing the importance of precision in sensitivity determination. Various models and approaches for FBG strain, temperature, pressure, displacement and acceleration sensors have been examined. Among these, FBG acceleration sensors (FBG accelerometers) present the most significant challenge due to the dynamic nature of the measured acceleration in terms of both magnitude and frequency. Studies have shown that sensitivity in these sensors is inherently frequency-dependent. The assumption of linear sensitivity within one-third or one-half of the resonant frequency can be improved through advanced methods, including machine learning techniques. By analysing both theoretical and experimental studies, this review highlights the critical factors affecting sensitivity accuracy and identifies areas where discrepancies may arise. The aim of the review is to provide a thorough understanding of the methods for achieving accurate sensitivity measurements in FBG accelerometers, thereby guiding future research and development in this domain.

1. An Overview of Optical Fibre Technology's History

The development of optical technology has a brief history that dates back to 1790 and the subsequent accounts shed light on its progression. Optical fibre is a technology for the interference-free transmission of light between the two ends of the fibre. As shown in Figure 1, the basic operation of an optical fibre includes light passing through a glass tunnel and reflecting back into the core when it comes into touch with the cladding. This phenomenon can come as a result of the optical fibre's structure, which enables light to bend around curves and traverse further distances without repeating itself.

* *Corresponding author*
E-mail address: firdaus@umpsa.edu.my

https://doi.org/10.37934/ard.129.1.164199

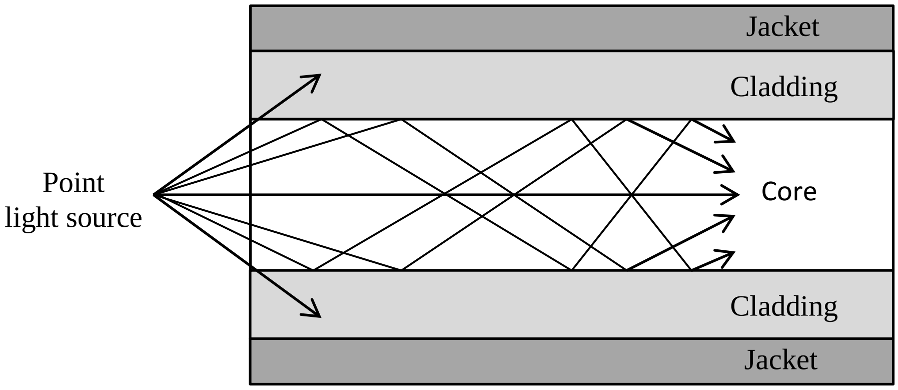

Fig. 1. Working principle of optical fibre [1]

In 1790, the Chappe brothers invented the optical telegraph tower in a line to transfer messages from one tower to the next tower 400 metres away, bringing in the era of optical communication [2]. In 1840, Daniel Collodon and Jacques Babinet demonstrated that light may be steered by refraction via a fountain's water stream [1]. In the decade that followed (1854), John Tyndall discovered that light could be twisted by directing it through curved, container-flowing water [3]. In 1927, John L. Baird and Clarence W. Hansell patented the concept of transmitting images for television or facsimile systems using arrays of hollow pipes or transparent rods [4]. In 1930, Heinrich Lamm demonstrated light transmission through a bundle of optical fibre with clear cladding for medical applications, but an unclad optical fibre could not transfer light well [3]. Abraham Van Heel revolutionised the optical fibre industry with his published documentation during the periscope project in 1954, yet this optical fibre was weak at transmitting light [3].

In 1954, Van Heel introduced the initial cladding element in optical fibre, which was constructed using bare glass that allowed for total internal reflection. Subsequently, Lawrence Curtiss developed cladding glass specifically for medical use in 1956, which later became known as the endoscope. Optical fibre with cladding glass suitable for medical purposes was introduced in 1960, although it lacked the necessary qualities for telecommunication applications [1]. Later on, Maurer, Keck and Schultz developed the first optical fibre (single-mode fibre) with new enhancement capabilities that have faster data transmission and minimum data loss for telecommunications [5] compared to traditional copper wire. Optical fibre was first employed in telephone field tests in 1977. After 1980, the breakthrough optical fibre technology began to appear in communications applications [3]. FBG is a novel optical fibre technology that can reflect certain wavelengths of light. With advancing technology in the field of optical fibre sensors, various types of sensors have emerged, including interferometer sensors, scattering fibre sensors, optical fibre gyroscopes, faraday rotation sensors and many others [6]. However, among these, significant research efforts have been dedicated to FBG sensors, with scholars exploring a wide range of parameters.

2. The Beginning of Fibre Bragg Grating Era

FBG technology functions by reflecting a certain wavelength of light known as the "Bragg wavelength" while letting the remainder of the signal travel through the fibre's end [7]. Bragg's law, which is applied in the FBG sensor, was discovered as a result of an experiment involving the introduction of radiation/x-rays into a crystal and the reflection of a certain intense peak of wavelength [8]. Hill made a significant discovery regarding optical fibre during experiments involving the use of argon-ion laser radiation on Germania-doped silica fibre [9]. These investigations revealed that after a minute of exposure to argon-ion laser radiation, the reflected light from the fibre increased. This observation led to the realization that the refractive index of the fibre's core was permanently changed. The phenomenon of the refractive index of the optical fibre increasing upon exposure to laser radiation is commonly known as photosensitivity. As a result of Hill's research, "Hill gratings" were developed to further explore this phenomenon [10]. Since then, researchers have worked to improve the manufacturing process through the close inscription of gratings onto optical fibres. This method can be divided into two categories: holographic [11] and non-interferometric [12]. To ensure the durability of the FBG sensor's reflectivity during production, the coating material must be eliminated from the optical fibres specified for grating writing [13]. Meltz *et al.,* [14] introduced a novel fabrication technique known as the interference writing method, as depicted in Figure 2(a). In this technique, the reflected laser radiation is divided into two beams and directed for five minutes onto the core fibre. The interference writing method for grating creation belongs to the category of holographic techniques and has demonstrated greater efficiency and adaptability than previous techniques. The resulting inscribed gratings have a reflectivity varying from 50% to 55% and exhibit remarkable resilience, remaining unaffected even after 18 hours of exposure to temperatures as high as 500°C. In an experiment conducted in 1990, Hill introduced the point-by-point writing method. Laser radiation is projected onto the core fibre point-by-point from one point to another, implying that the grating is being inscribed one at a time onto the core fibre (Figure 2(b)) [12]. The fibre is attached to the motor's shaft and with the motor's assistance, the grating is continuously written from one point to another (conveyor movement), regardless of whether the writing is moving or stationary. Nevertheless, writing on stationary is preferred. This procedure has the advantage of producing gratings of various lengths, spectral responses and periods [10]. According to Malo *et al.,* [15], the reflectivity of this writing technique is 70%.

Subsequently, Hill introduced the phase mask method for fabricating Bragg gratings, another innovative technique fibre (Figure 2(c)). In this technique, a phase mask made of laser-transmitting transparent silica glass is used [16]. The structure of the phase mask itself is corrugated, with the depth of the corrugations meticulously controlled to reduce diffraction effects. The phase mask is positioned near the optical fibre and laser radiation is directed onto it to imprint an interference pattern onto the fibre. The phase mask writing method simplifies grating inscription on optical fibres because it does not require stringent laser radiation conditions and only uses a single laser beam during the inscription procedure [17].

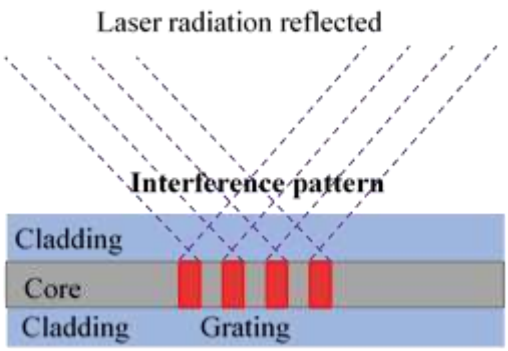

(a) Interference writing method

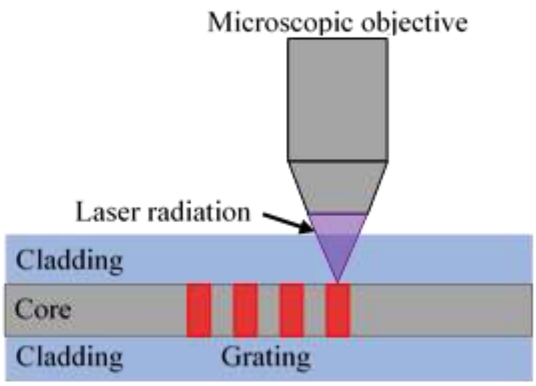

(b) Point-by-point writing method

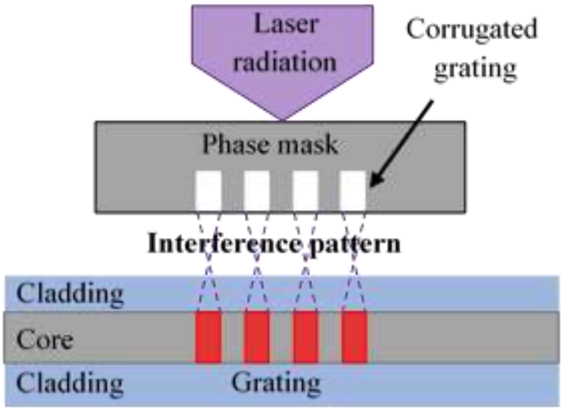

(c) Phase mask writing method

Fig. 2. Illustration of the writing methods of the grating

FBG stands out as a highly effective detection method in comparison to conventional electronic sensors due to its numerous advantages, including those associated with optical solutions such as immunity to electromagnetic fields, high-temperature survivability and corrosion resistance [18,19]. As depicted in Figure 3, the distributed Bragg grating is positioned within the cladding-coated core of the optical fibre [20]. The core functions as the path for light transmission between the two ends of the fibre, while the cladding, which has a lower refractive index, helps to minimise light loss along the path to the core.

There are two primary grating types: type I and type II. In type I gratings, the glass damage threshold is less than the index change, whereas it exceeds the index change in type II gratings [21]. Typical applications for Type I gratings include sensing, lasers and communications. Common varieties of structured gratings include uniform grating, chirped grating, tilted grating, long grating, discrete phase shift grating and superstructure grating [22]. Various physical parameters such as acceleration, displacement, pressure and temperature are measured using FBG technology. These measurements are derived from strain-induced variations in the Bragg wavelength [23].

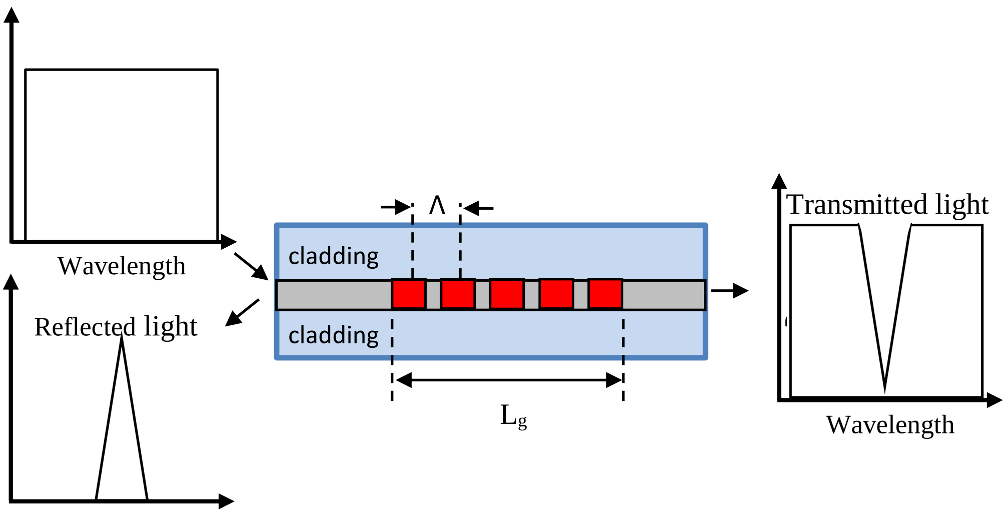

Fig. 3. Illustration of the principle of the reflection of Bragg's wavelength [20]

3. FBG in the Development of Sensors/Transducers

Fibre Bragg Gratings (FBGs) have emerged as versatile and powerful transducers in various fields of science and engineering, revolutionizing the way we measure and monitor physical parameters. These miniature optical devices are increasingly employed as sensors and transducers due to their remarkable ability to convert environmental changes into measurable optical signals. FBGs are particularly renowned for their precision, durability and suitability for applications in areas such as telecommunications, aerospace, civil engineering and healthcare. At its core, an FBG is a periodic variation in the refractive index of an optical fibre. This periodicity forms a grating structure within the fibre, typically achieved through a process of photosensitization. When illuminated with light, FBGs exhibit a unique spectral characteristic – they reflect a specific wavelength of light while allowing all others to pass through. This reflected wavelength, known as the Bragg wavelength, is determined by the period of the grating and the refractive index of the fibre core. When subjected to mechanical strain, temperature changes, pressure variations or other environmental factors, the Bragg wavelength of the FBG shifts accordingly. This shift can be detected with high precision using standard optical interrogation techniques.

3.1 FBG Accelerometer

In recent decades, accelerometers based on FBGs have attracted the interest of researchers and engineers as they are essential for vibration measurements. This is due to the success of FBG sensors in measuring strain, with the FBG strain sensor being the most successful [24], which has enabled the development of improved transducer designs that can also measure other fields, including acceleration. However, FBG sensors are very fragile by nature, so the use of a host is required for FBG sensors to function properly [19]. The FBG accelerometer is sensitive to cross-axis excitation, is bulky and is likely to suffer from the negative effects of birefringence caused by transverse strain leading to splitting of the FBG reflection peak, as it is based on an embedded grating method [25]. The beam and diaphragm structures are the two transducer structure types that are often used in FBG accelerometers for single-dimensional applications. A systematic classification of FBG accelerometers over a range of frequency frequencies is given in Table 1. This table illustrates how the operating frequency of the FBG accelerometer aligns within designated working frequency bands.

Table 1
Working frequency band classifications [26]

Working frequency bands (Hz)	Categories: Low/Intermediate/High
0 – 150	Low frequency
151 – 500	Intermediate-low frequency
501 – 800	Intermediate-high frequency
801 – 2000	High frequency

3.1.1 Diaphragm-type FBG accelerometer

As this thesis is being written, this section will review the published works on diaphragm-type FBG accelerometer over the previous four years. Li *et al.,* [27] introduced a cost effective and small extrinsic Fabry-Perot interferometer (EFPI) for acceleration measurement, which is constructed using a polyethylene diaphragm with a diameter of 10.0 mm. The experimental results demonstrate a recorded sensitivity of 135 mV/g (voltage sensitivity is used instead of wavelength shift sensitivity) over the range of 20 Hz to 1.5 kHz. Within this frequency range, the sensor has a constant frequency response, making it appropriate for use in micro vibration monitoring applications. In order to improve consistency between sensor units, Wang proposed a diaphragm-mass-collimator (DMC) integrated structure in his innovative fibre optic Fabry-Perot accelerometer (FPA) design [28]. This invention not only improves performance consistency, ease of manufacturing and compactness, but it also enhances the theoretical optimization of the sensor design. The sensitivity, resolution and dynamic range of the sensor are investigated using the proposed theoretical model. The deflectable diaphragm for the Fabry-Perot interferometer (FPI) for acceleration measurement was improved by Li *et al.,* [29] by integrating an aluminium-coated silicon wafer into the diaphragm structure. High consistency and manufacturing reproducibility are demonstrated by the fabrication of three fibre optic Fabry-Perot accelerometers (FOFPAs) with a measured average sensitivity of 2.6 V/g (100 Hz/3.2 kHz).

Li *et al.,* [30] proposed a high-sensitivity FBG accelerometer associated with theoretical model that combines the axial property of the optical fibre and the transverse property of a circular diaphragm by embedding a reflecting FBG sensor in a 0.6mm-thick diaphragm. Theoretical predictions and experimental findings were examined to confirm that the suggested theoretical model works as intended. In close agreement with the theoretical prediction of 422.4 pm/N, the experimental sensitivity was measured at 441.84 pm/N. Motivated by possibility of increased sensitivity, Liu *et al.,* [31] proposed a novel double diaphragms FBG accelerometer, with the FBG sensor embedded between two diaphragms. This dual-diaphragm arrangement enables both enhanced vibration signal accuracy and structural durability. A key aspect of the design is the additional secondary diaphragm, which reduces cross-axis sensitivity to under 2.1%, addressing a major limitation of previous accelerometers [32]. In comparison to earlier single-diaphragm designs targeting comparable frequency ranges, experimental testing revealed excellent sensitivity features, such as a broad flat response ranging from 50 to 800 Hz and high sensitivity from 23.8 to 45.9 pm/g. Furthermore, Liu *et al.,* [23] pursued additional improvements by introducing a figure of merit called "Product of Sensitivity and Resonant Frequency (PSRF)" to optimize overall performance. The key novelty lies in utilizing the PSRF figure of merit to enhance the design for high sensitivity while preserving a high resonance frequency and broadband response. As a result, it is highly suitable for applications demanding high resolution over a broad bandwidth, such as seismic and vibration monitoring. By implementing this approach, they can improve their previous design presented in [31,32] to reach a maximum flat sensitivity range of 152.0 pm/g and a resonant frequency of 441.0 Hz. Another study by Liu *et al.,* [33] that also focuses on a figure of merit, wherein the proposed FBG accelerometer exhibits higher sensitivity and reduced cross-sensitivity. The sensitivity range spans from 754.3 to 763.2 pm/g within the flat region, showcasing superior small signal detection capabilities.

Fan *et al.,* [34] introduced a distinctive FBG accelerometer mechanism by integrating the concepts of a diaphragm and cantilever in their innovation. Three equal-length cantilever beams are symmetrically neatly cut and placed onto the diaphragm. These three suspension beams support the copper inertial mass block located in the middle of the diaphragm. The experimental findings indicate that the accelerometer's flat frequency response spans from 5.0 to 60.0 Hz, with a natural frequency of 90 Hz and an acceleration sensitivity of 485.75 pm/g.

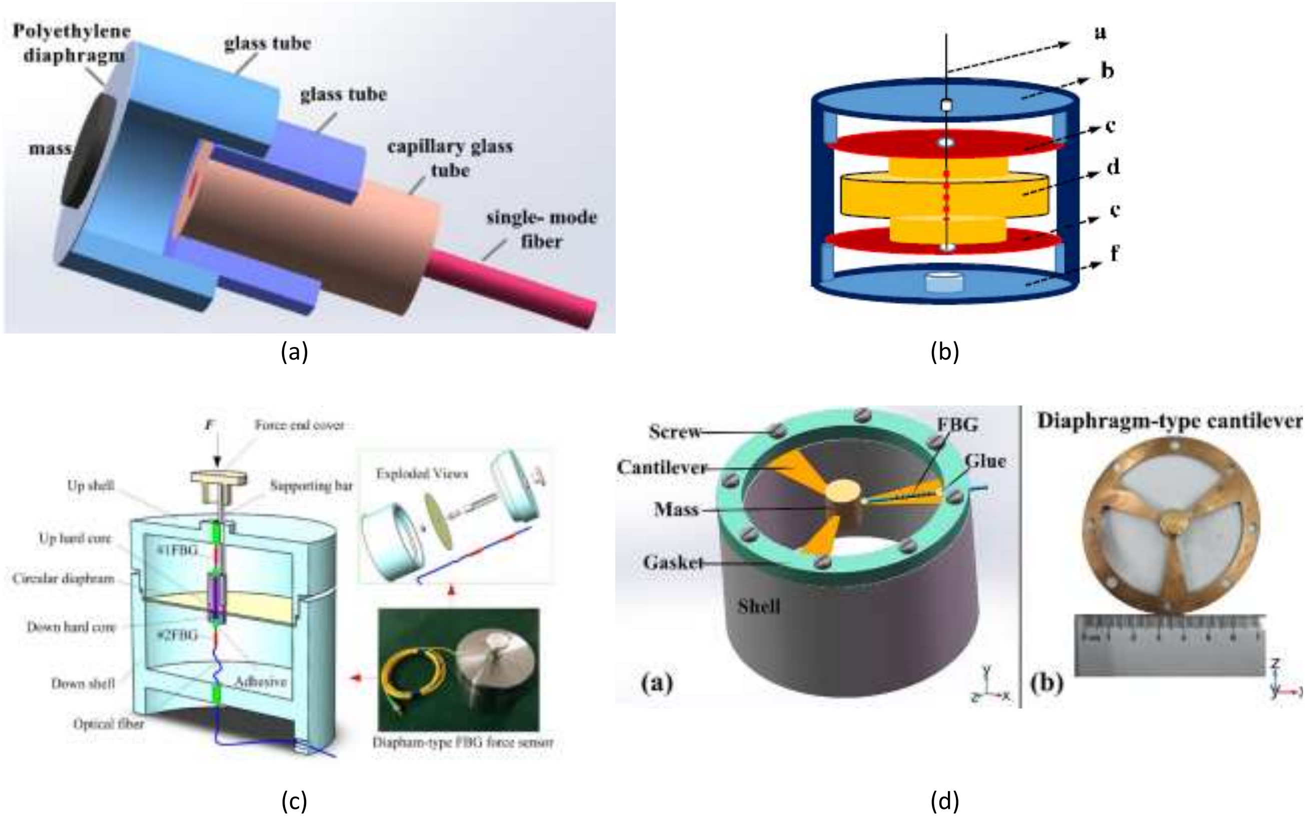

Fig. 4. Several examples of diaphragm-type FBG accelerometers (a) [27] (b) [23] (c) [28] (d) [34]

Integration of diaphragm and additional structural elements is demonstrated in the work of Zhang *et al.,* [35]. They employed a novel approach by integrating double diaphragms with H-shaped hinges. Theoretical and experimental analyses affirm the effectiveness of this integrated h-shaped hinge structure in significantly enhancing the sensitivity and resolution of the broadband FBG accelerometer. Table 2 depicts several diaphragm-type FBG accelerometers and their sensitivity, techniques used and application.

Table 2
Several diaphragm-type FBG accelerometers

Reference	Technique	Sensitivity	Application
[27]	polyethylene diaphragm	135 mV/g	Micro vibration monitoring
[28]	diaphragm-mass-collimator (DMC)	Not given	Not given
[29]	aluminium-coated silicon wafer - diaphragm	2.6 V/g	Micro vibration monitoring
[30]	circular diaphragm	441.84 pm/N	Precision test platform, aerospace equipment
[31]	two diaphragms	23.8 to 45.9 pm/g	Not given
[23]	two diaphragms (figure of merit concept)	152.0 pm/g	Not given
]33]	two diaphragms (figure of merit concept)	754.3 to 763.2 pm/g	Not given
[34]	three equal-length beams on a diaphragm	485.75 pm/g	Not given
[35]	diaphragm and h-shaped hinge	Not given	Not given
[36]	A single diaphragm without inertia mass	9.64 pm/g	Small structure measurement

3.1.2 Cantilever-type FBG accelerometer

It was found that the most common beam structure used in the FBG accelerometers for single-dimensional applications is based on cantilever beam mechanism [37-46]. However, many researchers also already starting to investigate two-dimensional and three-dimensional applications of FBG accelerometer [47-49]. The cantilever based FBG accelerometers principally include of a vibrating cantilever with a FBG bonded on the surface or attached to it. The bending strain of the cantilever is transmitted to the FBG, resulting in a wavelength shift proportional to the strain. The bending strain of the cantilever is proportional to the vertical acceleration and the FBG wavelength shift is a direct measure of the vertical acceleration.

The most recent study of a cantilever-based FBG accelerometer is done by Nguyen *et al.,* [50]. The research is introduced an innovative FBG accelerometer featuring a V-shaped flexure hinge structure with enhanced sensitivity. Theoretical calculation and simulation analysis software were employed to evaluate the proposed structure's parameters. Experimental results show a sensitivity of approximately 67.9 pm/g under a working bandwidth of 400–900 Hz and a resonant frequency of 1250 Hz. The influence of temperature at 8.4 pm/◦C and transverse interference validate 3.5%. These findings align with simulations, affirming the sensor's performance. This innovation holds promise for enhancing structural integrity monitoring in large-scale structures by detecting medium- and high-frequency vibration measurements. With a simpler design of the FBG accelerometer, Korayem *et al.,* [94] investigated the structure of the single cantilever beam FBG accelerometer with a mass block at its tip. The mass block is suspended at a certain height within an encasing structure. FBG is positioned and fixed perpendicular to the surface of the vibrating cantilever beam through a hole made in the encasing structure. The influence of the cantilever beam parameters on the natural frequency and sensitivity are discussed through simulation and laboratory calibration with vibration exciter. The test results show that the optimized system has a resonance frequency of 75 Hz within a measuring range of 5–55 Hz and high sensitivity of ±433.7 pm/g. From the field test in comparison with the 4.5 Hz vertical geophones, found that the first arrival time of both systems is perfectly matching. Hence, this sensor system has the potential to monitor active signals. On the same year, Qiu *et al.,* [51] also researched the similar types of the accelerometer yet the structure of accelerometer is focused on the miniaturized symmetrical cantilever beam. By using formula derivation and Analysis of System (ANSYS) simulation software, the structural parameters of the sensor are optimized and simulated for analysis. According to the simulation results, the real sensor is made. Finally, the sensor performance is tested and the results show that the natural frequency of the sensor is about 72 Hz, which can be used to monitor vibration signals in the frequency range of 8–52 Hz. The sensitivity of the sensor is about 681.7 pm/g and the resistance to transverse interference is less than 4.9%. Its volume is only 6.48 cm^3, which is much smaller than that of an FBG accelerometer of the same kind.

A study on a high-sensitivity FBG accelerometer with the application for flow monitoring in oil wells was carried out by Jiang *et al.,* [52]. Two fibre supports are arranged at both ends of a cantilever beam; therefore, the FBG can be stretched longitudinally by both displacement and rotation of the free end. The theoretical model of the sensitive structure is abstracted by the elasticity theory approach, which is verified by the simulation results. The difference between the simulation and theoretical results is 9.4 %, indicating that the theoretical derivation process is sufficiently accurate. Additionally, the influence of key structural parameters is analysed for structural optimization. The experimental results show that the accelerometer exhibits a resonant frequency of approximately 76 Hz, an average sensitivity of 59.3 dB re pm/g for a 1–60 Hz flat response interval and a cross-sensitivity of less than –24.43 dB (<6.1 %), which is capable of low frequency and precision vibration measurements. Similarly with Jiang *et al.,* [52], Wu *et al.,* [53] also focused on designing a high-frequency and high-sensitivity acceleration sensor based on FBG. The sensor adopts a double cantilever structure to sense the vibration perpendicular to the axis. Compared with a single cantilever structure, the natural frequency is increased without reducing the sensing length. As a result of the structure design and material selection, the sensor shows a high natural frequency of 8658 Hz and its sensitivity is 0.44 pm/g. After the photoelectric demodulation is used, the sensitivity is 52 mV/g and the linearity is 0.998.

Lim *et al.,* [54] proposed the vibration measurement system by using seven low-frequency cantilever-based FBG accelerometers (CFA) for a suspension bridge and obtaining three natural vibration frequencies of 1.15 Hz, 1.54 Hz and 3.17 Hz. Each accelerometer has an end-loaded cantilever beam, specifically tailored to achieve a uniform sensitivity for a frequency range of 1 to 4Hz and as a result, the average vibration sensitivity is 0.562 nm/G with a small standard deviation of ~5% has been measured. This investigation has shown the feasibility of the proposed measurement system for determining the mode shapes and dynamic frequency analysis of a suspension bridge. It is a potential method for structural health monitoring for other similar civil structures. An acceleration sensor based on FBG that can be used in downhole for a long time was done by Li *et al.,* [55]. The acceleration sensor uses the inertial force generated by the mass to make the symmetrically tilting cantilever beams bend slightly to detect the vibration signal. The operating frequency range of the acceleration sensor is from 0.1 Hz to 30 Hz, the sensitivity is 290 pm/g at room temperature and the maximum lateral interference degree is 3.6%. Most importantly, the sensor packaged by glass welding can keep excellent stability under long- term high temperature. Moreover, the sensor has a quick response to severe temperature shock and can maintain measuring accuracy after cyclic thermal shocks. Therefore, the sensor can be reliably used for micro-vibration measurement in harsh environments such as downhole. Next, study done by Jia *et al.,* [47] focusing on two-dimensional cantilever vibration sensor based on FBG. The sensor consists of a section of optical fibre with double FBGs and three different beams. After theoretical analysis and experimental verification, the proposed sensor has a high sensitivity response. The experimental result shows that the natural frequency of the sensor in the *x/y* direction of vibrations is respectively 505/177 Hz while the sensor's sensitivity is respectively 125.85/82.32 pm/g in the *x/y* direction of vibration. The proposed sensor has great potential for application in two-dimensional vibration signal detection of bridges, roads and buildings.

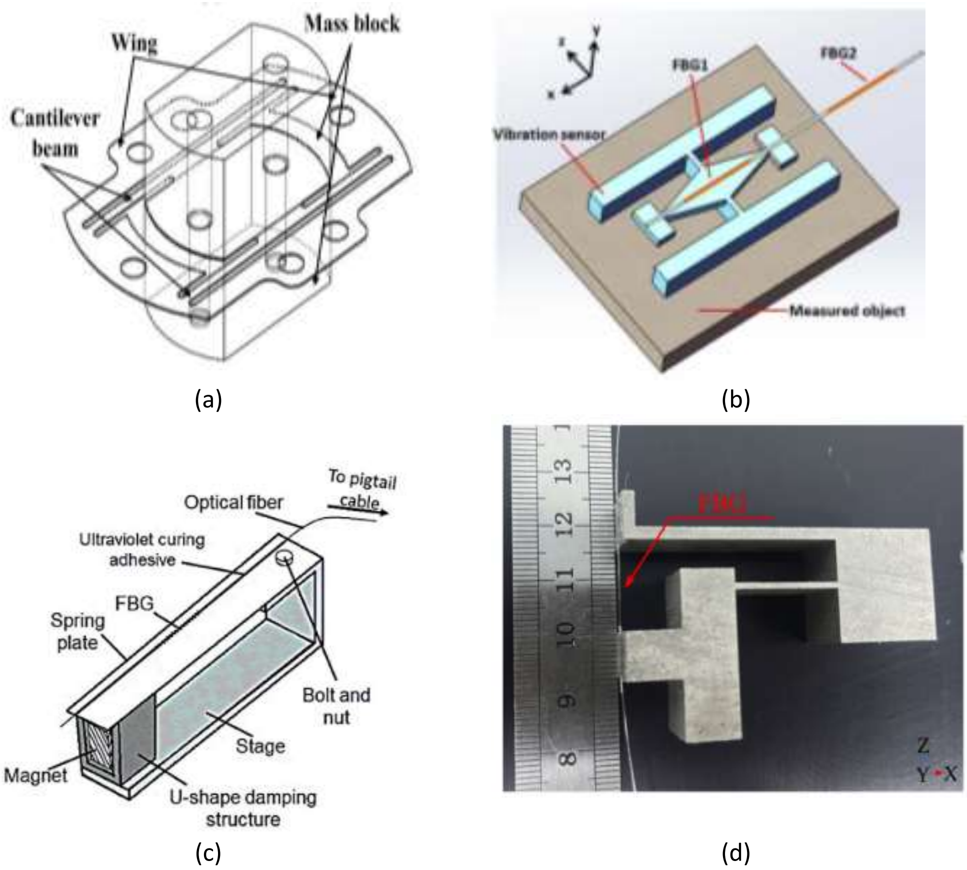

Fig. 5. Several examples of cantilever FBG accelerometers (a) [51] (b) [53] (c) [55] (d) [56]

Parida *et al.,* [57] presented a novel double-L cantilever-based FBG accelerometer. Test results are found to be closely matching with the analytical and FEM simulation results. The FBG accelerometer has a linear operating range of ±6 g. A high sensitivity of 406.7 pm/g is demonstrated with an excellent linearity of 99.86%. A very low cross-axis sensitivity of 2.2 pm/g is achieved. The accelerometer has a natural frequency of 86 Hz with an operating frequency range from 5 Hz to 50 Hz, where the response remains relatively constant. Self-temperature compensation is achieved with a very low-temperature sensitivity of 0.016 pm/◦C. The overall performance achieved for the proposed FBG accelerometer is better than other FBG accelerometers of comparable dimensions. Different with Parida *et al.,* [57] and Yang *et al.,* [58] demonstrated a thorough analysis of the performance of different strain magnification structures with FBG by using four kinds of cantilever beams with different shapes. Simulation results show that the strain magnification structures of the different cantilever beams are different. There is a positive and linear correlation between the displacement of the free end of the cantilever beam and the average strain at the pasting position of the FBG. The correlation is used to calculate the displacement sensitivity and analyse the efficacy of the different strain magnification structures. From the experiment results, the average values of the displacement sensitivities for the different beam shapes were 120.6 pm/mm, 321.9 pm/mm, 258.4 pm/mm and 310.5 pm/mm, respectively while the theoretical prediction are 102.3 pm/mm, 272.8 pm/mm, 229.4 pm/mm and 261.1 pm/mm, respectively. There is a reasonable agreement between simulation and experiment, which shows that the efficacy is related to the increasing rate of the average strain over the FBG length. Feng *et al.,* [59] investigated on FBG accelerometer based on a hybridization of two cantilever beams. The experimental results show that the proposed sensor exhibits a high dynamic sensitivity of 218.4 pm/g and broad frequency range of 10–150 Hz with a wide dynamic range of 0.1 to 3 G. The cross-axis response is 3.2% of the main axis and the temperature is self-compensated owing to the same responses to temperature of two reflection wavelengths. In real seismic applications, the proposed device is expected to achieve an ideal response with further parameter optimization and suitable package. Table 3 depicts several cantilever FBG accelerometer and its sensitivity, techniques used and application.

Table 3
Several cantilever FBG accelerometers

Reference	Technique	Sensitivity	Application
[50]	V-shaped flexible hinge	67.9 pm/g	Vibration monitoring in large-scale structures
[37]	Cantilever beam FBG accelerometer with mass block at its tip	±433.7 pm/g.	Vibrations monitoring from active seismic sources in the external environment.
[51]	Symmetrical Cantilever Beam	681.7 pm/g	Vibrations monitoring from large-scale engineering structures
[60]	Two fibre supports at both ends of a cantilever beam	59.3 dB re pm/g	Flow monitoring in oil wells
[53]	Double cantilever structure	52 mV/g	Not given
[54]	Cantilever-based FBG accelerometer array	0.562 nm/g	SHM for suspension bridge and other similar civil structures
[55]	Symmetrical tilting cantilever beams	290 pm/g	Micro vibration monitoring
[47]	Two-dimensional cantilever beam	125.85 pm/g in the x direction 82.32 pm/g in y direction	Two-dimensional vibration signal detection of bridges, roads and buildings
[59]	Hybridization of two cantilever beams.	218.4 pm/g	Real seismic applications
[56]	Equal-section cantilever beam in combination with the lever amplification principle	239.12 pm/g	Not given
[60]	Changing the base of cantilever FBG accelerometer	134.29 pm/g	Oil and gas exploration
[38]	FBG perpendicular to the cantilever surface	330 pm/g	Not given

4. Mathematical Modelling of Cantilever FBG Accelerometer

It has been noted that not all research on cantilever FBG accelerometers that focus on features such as dynamic response, linearity and accuracy, sensitivity, vibration mode and frequency, include both simulation and experiments. In simulation studies to predict the behaviour of cantilever FBG accelerometers, researchers typically proposed specific mathematical models based on the configuration of its mechanism to understand the accelerometer's response. In this subsection, the investigation exclusively centres on the mathematical model of the cantilever FBG accelerometer, with a specific focus on the important elements, notably strain and sensitivity equations. The researcher has both derived and employed these equations in their study. In addition, it should be mentioned that the specifics of the derivation will not be covered in this sub-section.

Fuhr *et al.*, [61] established a static relationship between fluctuations in applied load, *F* and strain $\varepsilon(x)$ (Figure 6) and detailed how the strain of FBG may be calculated using pure bending theory [62]. The strain $\varepsilon(x)$ is given by Eq. (1):

$$\varepsilon(x) = 12\frac{F(l-x)v(x)}{E_a b(x) t^3(x)} \tag{1}$$

Where, E_a is Young's modulus of the material, $b(x)$ is the beam width, $t(x)$ represents the beam's thickness and $v(x)$ is the distance from the midplane. It is noted that the resulting strain depends solely on the applied load and is not influenced by acceleration. If other parameters, such as $b(x)$, $t(x)$ etc. are held constant, the sensitivity of the FBG accelerometer is solely governed by the applied load, remaining linear and consistent irrespective of the magnitude of the applied load, whether it is small or large.

Successively, other scholars [40,42,43,45,63,64] adopted this approach for dynamic study, in which the static force is substituted by base acceleration, *a*, known as the single-degree-of-freedom (SDOF) model. The core principle of this model is that the base excitation is time-harmonic. The equation of motion, for instance, is taken from Basumallick *et al.,* [40], the strain and sensitivity of the cantilever FBG accelerometer is given as in Eq. (2) and (3):

$$\varepsilon(x) = \frac{3(0.5d+d_f)(l-x)v(x)}{(\omega_n^2-\omega^2)l^3} \times a \tag{2}$$

$$S = \frac{1.2\times\varepsilon(x)}{a} \tag{3}$$

Where, these parameters (strain and sensitivity) being dependent on both the resonant frequency, ω_n and excitation frequency.

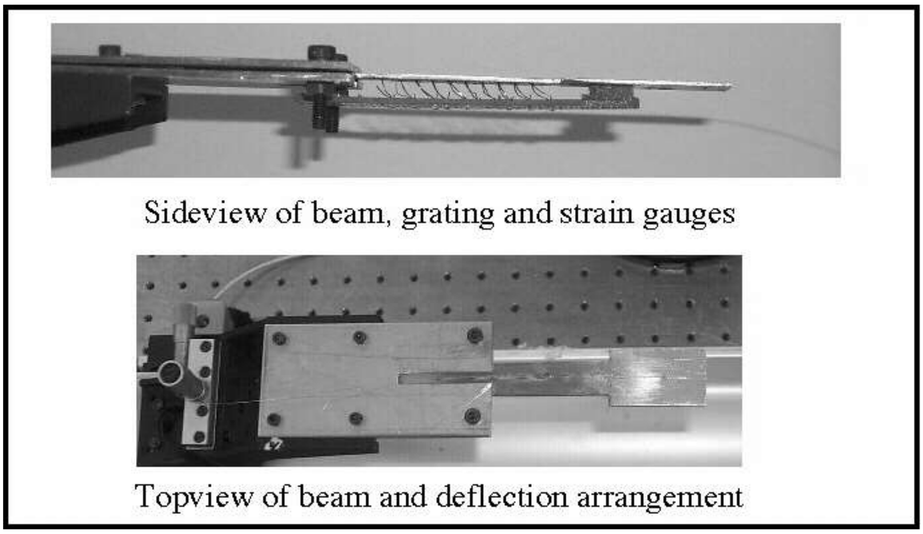

Fig. 6. Cantilever FBG accelerometer proposed by Fuhr *et al.,* [61]

The semi-circular cantilever FBG accelerometer (Figure 7) proposed by Zhang *et al.,* [65] employs a simplified model where the strain is solely dependent on the axial deformation of the fibre, denoted as ΔL, in relation to the effective length of the fibre, represented by L (Eq. (4)). Its sensitivity is exclusively governed by constant parameters, including the effective elastic-optic coefficient P_e, the center wavelength of the back-reflected light λ_B, the mass of the cantilever beam m, the equivalent elastic constant K and the effective length of the fibre L (Eq. (5)). Notably, this sensitivity is independent of the excitation frequency or acceleration, highlighting the model's inherent simplicity and efficiency.

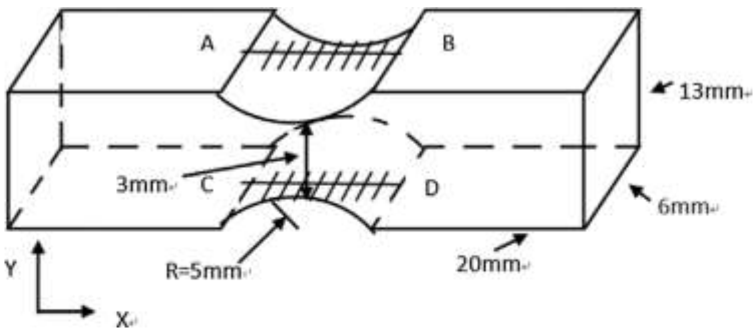

Fig. 7. Double-semicircle cantilever FBG accelerometer proposed Zhang *et al.,* [65]

$$\varepsilon = \frac{\Delta L}{L} \tag{4}$$

$$S = \frac{(1-P_e)\lambda_B m}{KL} \tag{5}$$

Casas-Ramos *et al.,* [66] have introduced another mathematical model that draws upon superposition methods introduced by Gere *et al.,* [67] as in Eq. (6) and (7). This model establishes a linear dependence of strain on the mass, dimensions and mechanical properties of the cantilever. As illustrated in Figure 8, the strain and sensitivity of the proposed sensors remain constant irrespective of the applied force, acceleration or excitation frequency of the FBG accelerometer.

$$\varepsilon = \frac{M\left(2L_2^3 I_2 + I_1 L_1\left(L_1(2L_1+3L_2)+3L_2(L_1+2L_2)\right)\right)}{6E_{AL}I_1 I_2 L_3} \times g \tag{6}$$

$$S = \lambda_B(1-P_e)\frac{\varepsilon}{g} \tag{7}$$

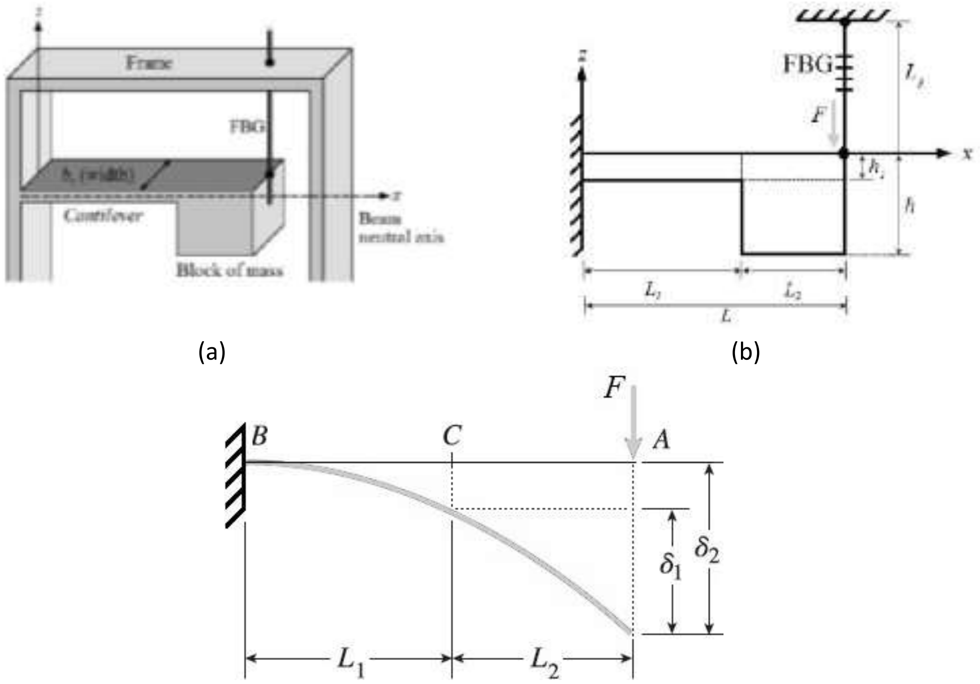

Fig. 8. Cantilever FBG accelerometer with a block mass [66]

Parida *et al.,* [57] introduce a straightforward mathematical model to represent their cantilever FBG accelerometer (Figure 9), despite the inherent complexity of their innovation's structure. This model is also depending by the dimensions, mechanical properties and dynamic characteristics of the host, including natural frequency and stiffness. As depicted in Figure 9, the strain and sensitivity of their innovation are expressed by Eq. (8) and Eq. (9). Noted that L_f is length of sensing fibre, H and L are height and length of each *L*-cantilever, M is mass of the cantilever and K_1 and K_2 are stiffness of sensor head and sensing fibre, respectively.

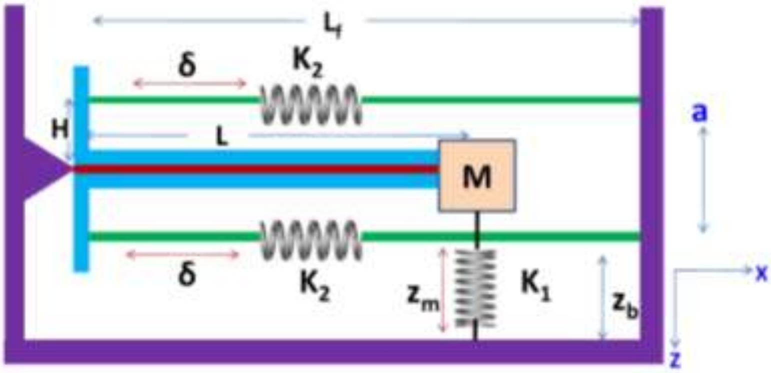

Fig. 9. Double-L cantilever FBG accelerometer [57]

$$\varepsilon = \frac{A}{4\pi^2 L_f f_n^2}\left(\frac{H}{L}\right) \tag{8}$$

$$S = \frac{M}{L_f\left\{K_1 + 2K_2\left(\frac{H}{L}\right)^2\right\}}\left(\frac{H}{L}\right) \tag{9}$$

Considering *y*-direction of the two-dimensional cantilever FBG accelerometer proposed by Jia *et al.,* [47], its mathematical modelling relies on the beam deflection theorem. The strain (Eq. (10)) is a function of the effective length of the fibre l and the deflection of the mass block y, as illustrated in Figure 10. Meanwhile, the sensitivity (Eq. (11)) is a function of the strain ε, the center of wavelength of FBG1 λ_1, the effective elastic-optic coefficient P_e, the equivalent mass of the sensor M, the initial strain of optical fibre under the action of gravity ε_0, the Young's Modulus of the fibre E_f, the cross-sectional area of the fibre A_f and the equivalent stiffness of cantilever beam, K_{neff}. Notably, there is no explicit indication clarifying whether both equations are dependent on acceleration or the excitation frequency.

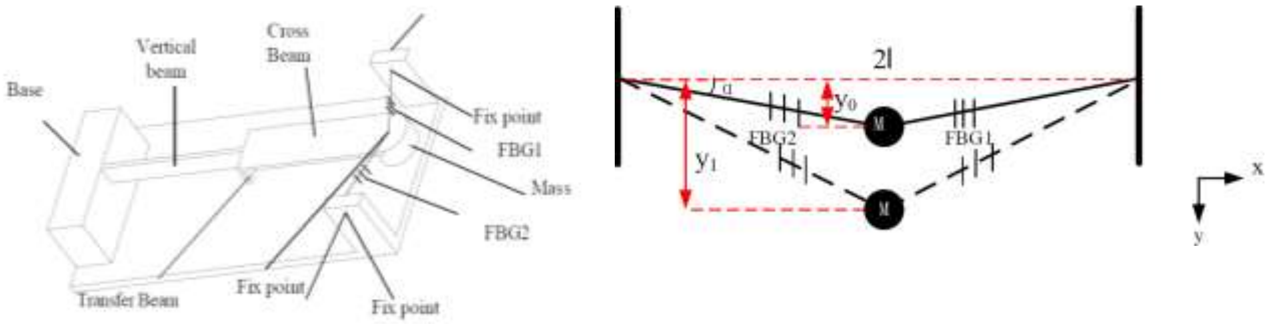

Fig. 10. Two-dimensional cantilever FBG accelerometer [47]

$$\varepsilon = \frac{\sqrt{l^2+y^2}-l}{l} \tag{10}$$

$$S = 2(1-P_e)\frac{\varepsilon\lambda_1\sqrt{\varepsilon_0^2+2\varepsilon_0}}{2E_fA_f\varepsilon_0+lK_{neff}(\varepsilon_0+1)} \tag{11}$$

By adding two block masses onto the cantilever (Figure 11), Wang *et al.,* [68] adopt the SDOF model as proposed by Fuhr *et al.,* [61]. However, the model by Wang yields only half of the results produced by the SDOF model (Eq. (12)), due to different configuration of beam and block masses. However, the strain produced by the FBG sensor is indeed proportional to the strain generated by the beam, as elucidated by the Eq. (12). The sensitivity of the cantilever FBG accelerometer, however, is solely dependent on the dimensions and mechanical properties of the structure, the effective elastic-optic coefficient and the original central wavelength of the fibre, as specified in Eq. (13).

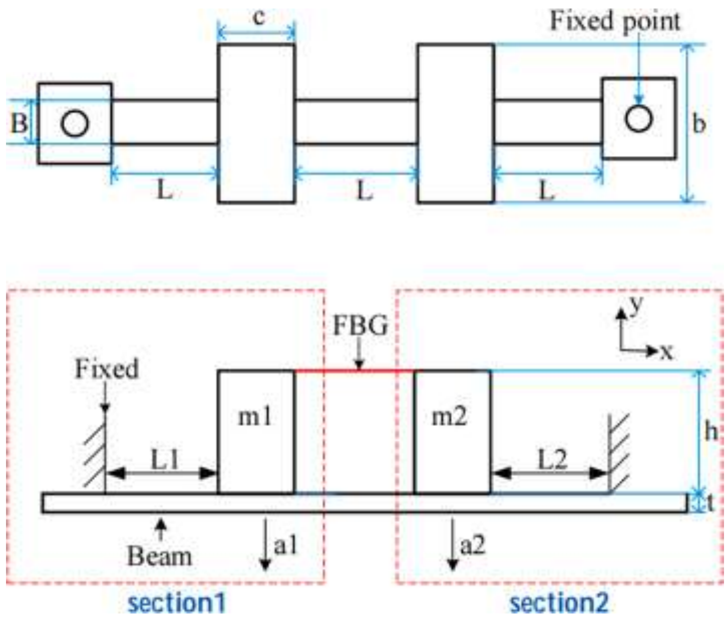

Fig. 11. Two block masses cantilever FBG accelerometer [68]

$$\varepsilon_{FBG} = \frac{\varepsilon\left(\frac{t}{2}+h\right)}{\frac{t}{2}} \tag{12}$$

$$S = (1-P_e)\frac{t+2h}{t}\frac{6m_1}{EBt^2}L_1\lambda_0 \tag{13}$$

Similar to the concept presented by Wang *et al.,* [68], although with a slightly different mechanism, Qiu *et al.,* [69] employed the concept of the moment of the cantilever into the mathematical model of their cantilever FBG accelerometer (Figure 12). The resulting strain and sensitivity are expressed in Eq. (14) and Eq. (15), respectively, both of which depend on the angle of deflection of the beam and the base acceleration.

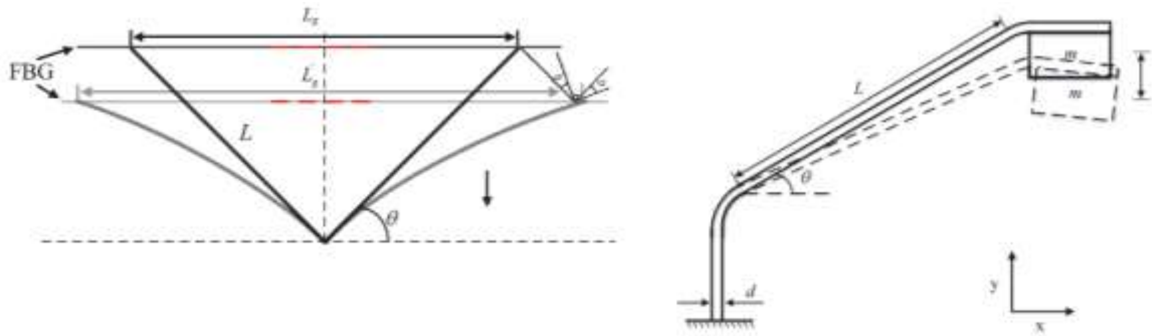

Fig. 12. Double titled cantilever FBG accelerometer [69]

$$\varepsilon = \frac{2\alpha(L+2\nu\sin\theta)\cos\alpha}{L\ \sin 2\alpha} - 1 \tag{14}$$

$$S = \frac{S_\varepsilon \varepsilon}{a} \tag{15}$$

In short, considering only a simple cantilever FBG accelerometer consist of single beam with and without tip mass studied by Basumallick *et al.,* [40,63], Gagliardi *et al.,* [42], Zhang *et al.,* [45] and Zhu *et al.,* [64], the mathematical model employed does not take into account for the base excitation of the cantilever beam, which is subject to small translation and rotation. Furthermore, the beam response for SDOF exhibited a linear pattern along the beam when shear force was equated to zero for the pure bending model. Because of that, Khalid *et al.,* [70,71] introduced a modal model of the cantilever Euler-Bernoulli (EB) beam into the wavelength shift equation for both single beams with (namely FBG-MMTP) and without tip mass (FBG-MM). This model has proven to be convincing when validated against experimental wavelength shift data. As depicted in Figure 13, the strain and sensitivity derived from this model are expressed by Eq. (12) and Eq. (13) for FBG-MM and Eq. (16) and Eq. (17) for FBG-MMTP, respectively.

$$\varepsilon_{FBG}(x,t) = -(h + h_f)\frac{\partial^2 u_{rel}(x,t)}{\partial x^2} \tag{16}$$

Where,

$$\frac{\partial^2 u_{rel}(x,t)}{dx^2} = 2U_0 e^{i\omega t}\sum_{r=1}^{\infty}\left(\frac{\lambda_r}{L}\right)^2\left(\left[cosh\frac{\lambda_r}{L}x + cos\frac{\lambda_r}{L}x - \sigma_r\left(sinh\frac{\lambda_r}{L}x + sin\frac{\lambda_r}{L}x\right)\right]\frac{\sigma_r}{\lambda_r}\frac{\omega^2}{\omega_r^2 - \omega^2}\right)$$

$$S = \frac{1.2\times\varepsilon_{FBG}}{\ddot{u}_b(x,t)} \tag{17}$$

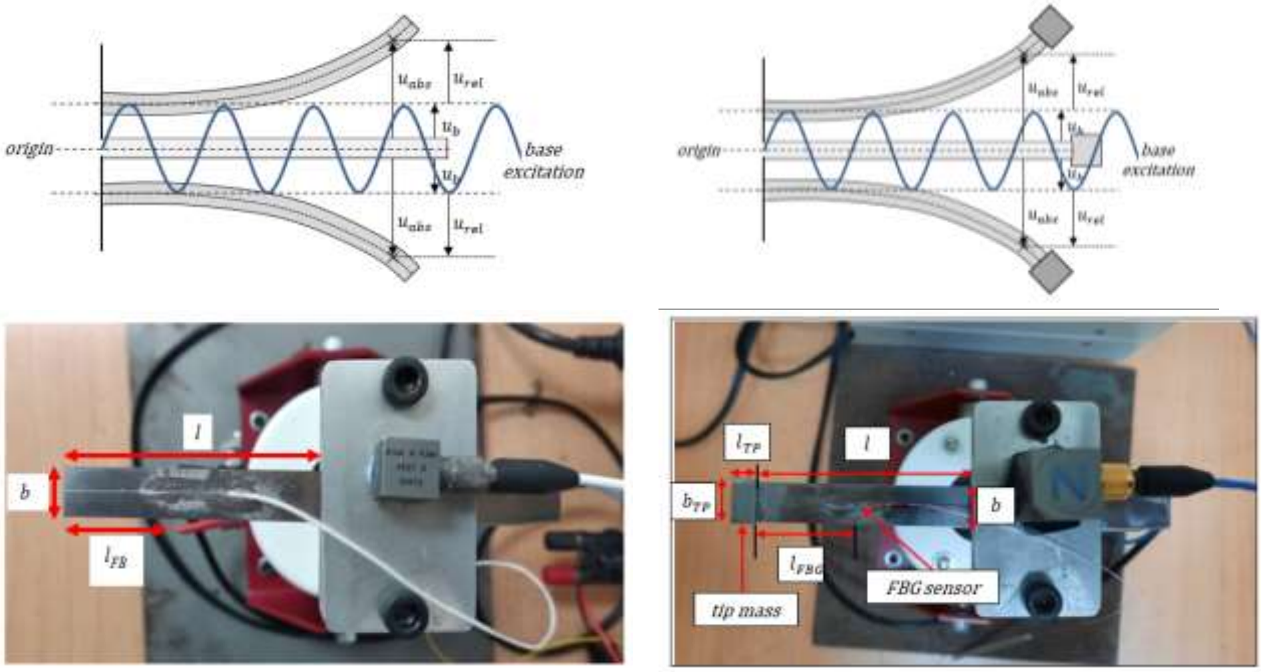

(a) (b)

Fig. 13. Single cantilever FBG accelerometer with (a) without [70] (b) tip mass [71]

5. Sensitivity and Wavelength Shift Plots of Cantilever FBG Accelerometer Obtained from Experimental Works

In the investigation of FBG accelerometer performances, researchers primarily employ two approaches: actual on-site tests e.g., [37] and experimental works e.g., [39,47]. In the latter approach, a shaker is employed to induce the base acceleration for the FBG accelerometer, resulting in responses in the form of wavelength shift. This wavelength shift is then analysed and compared, sometimes in comparison with voltage-based accelerometers like piezoelectric accelerometers.

In the experiment works, the methodology employed in prior studies serves as a basis for the experimental framework in the thesis. It is related to the excitation frequency range that is being employed, whether it is a broad sweep across multiple frequencies or if it revolves around a single frequency. Focusing on sensitivity studies, the most criterion in the development of a FBG accelerometer lies in the operating frequency range it can effectively cover. The operating frequency range that is used to calculate sensitivity in the most of experimental investigations is basically less than one-half or one-third of the resonant frequency of the FBG accelerometer. In addition to operating frequency range, given the FBG accelerometer is very sensitive to strain, the excitation of the FBG accelerometer using a swept signal over the frequency range is not a commonly adopted practice. The common practice is to excite the FBG accelerometer at a single excitation frequency during each time, at a specific frequency interval.

To investigate the response of the FBG accelerometer at its resonant frequency, the excitation frequency range is extended beyond the linear frequency range. The linear operating frequency range is typically determined by observing a steady and gradual increase in sensitivity or wavelength shift after plotting them against excitation frequencies. To prevent confusion, it is important to note that in this study, some researchers present their results by plotting sensitivity against excitation frequencies, while others plot wavelength shift against frequencies. Despite this difference in presentation, both plots lead to the same conclusion regarding whether the response of the FBG accelerometer is frequency-dependent or not. Another important point to understand is that when the plot gradually increases, it does not necessarily mean the sensitivity is constant. Instead, it indicates that at different excitation frequencies, with the same level of acceleration, sensitivity either increases or fluctuates.

In an effort to improve sensitivity, experimental work was conducted by Basumallick *et al.,* [40] at a frequency range of 5 to 30 Hz, employing an interval frequency of 2 to 5 Hz and maintaining a constant acceleration of 1g. The linear operating frequency was not mentioned in the study. Nguyen *et al.,* [50] also employed a single excitation frequency at each instant, with a 100 Hz interval, ranging from 400 to 900 Hz. They assumed that the sensitivity would average 67.9 pm/g in the linear operating frequency range of 400 to 900 Hz; however, as shown in Figure 14(a), the sensitivity plot demonstrates that this value fluctuates throughout these frequencies. As depicted in Figure 14(b), Feng *et al.,* [55] demonstrate that their analysis reveals fluctuations in the wavelength shift across the excitation frequency range of 0 to 30 Hz. Additionally, they employed a singular excitation frequency at a given instance, ranging from 0.1 to 100 Hz with intervals of 5 Hz. Qiu *et al.,* [51] illustrate an increase in wavelength shift with excitation frequencies ranging from 0 to 100 Hz, at intervals of 2 Hz and a maximum acceleration of 0.1g, as depicted in Figure 14(c). Notably, a linear operating frequency range of 8 to 52 Hz was chosen, revealing large differences for frequencies below 8 Hz. Parida also only uses a single excitation frequency at a time, ranging from 5 to 150 Hz with 5 Hz intervals and found that the linear operating frequency ranges from 5 to 50 Hz where the wavelength shift linearly increases, as shown in Figure 14(d) [57].

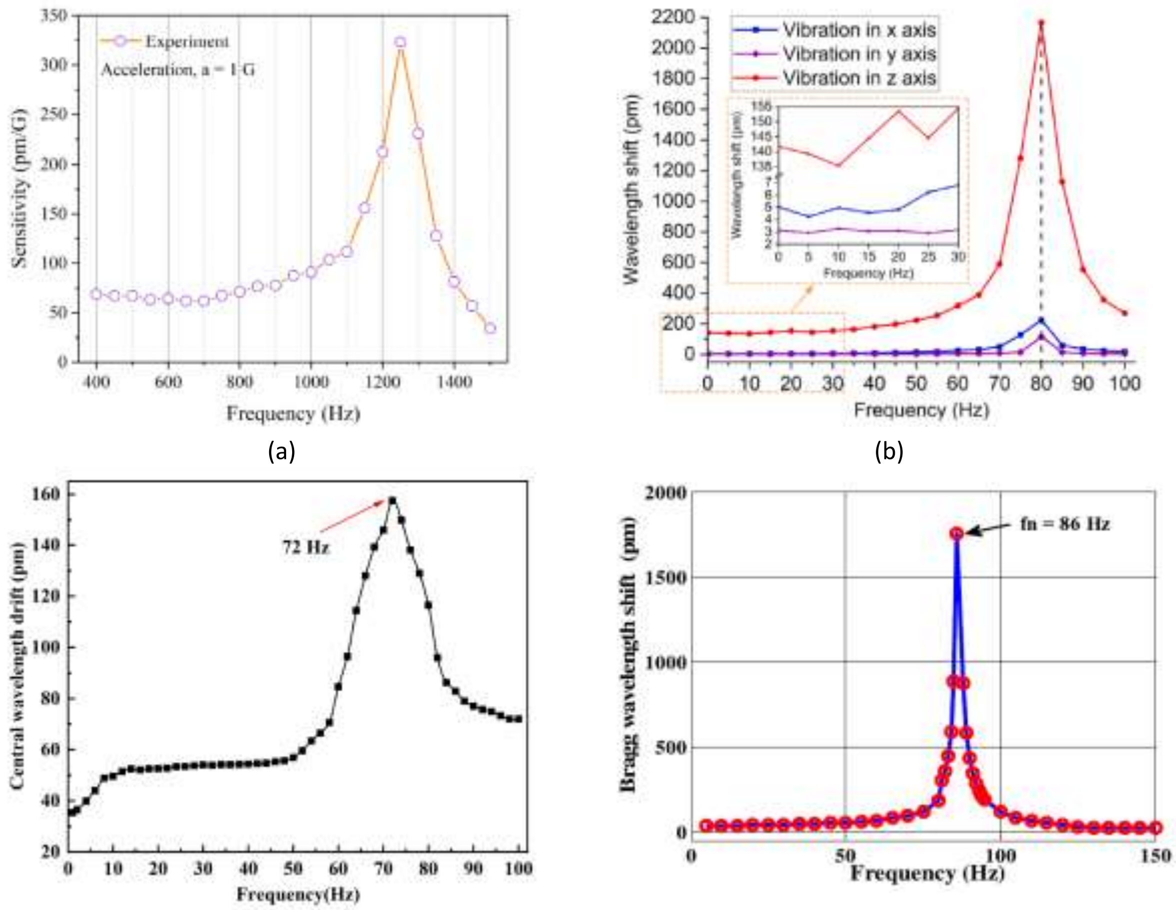

(a) (b) (c) (d)

Fig. 14. Sensitivity/wavelength shift plots (a) [50] (b) [55] (c) [51] (d) [57]

In another study conducted by Feng *et al.,* [59] (Figure 15(a)), a single excitation frequency is also employed at a time, with the excitation frequencies ranging from 5 to 400 Hz and a 5 Hz interval, all under an acceleration of 1.5g. The resonant frequency is determined to be at 210 Hz and the linear operating frequency range spans from 5 to 150 Hz. Other studies by Jiang *et al.,* [60], Zhang *et al.,* [65] and Wang *et al.,* [68] show a small change (either increase or decrease) of sensitivity or wavelength shift of the FBG accelerometer within its linear frequency range, as shown in Figure 15(b), 15(c) and 15 (d). Notably, all these studies employ a single excitation frequency at each instance. Jiang *et al.,* [60] and Zhang *et al.,* [65] specifically focus on low-frequency FBG accelerometers, with linear operating frequency ranges of 2 to 60 Hz and 0 to 25 Hz, respectively. In contrast, Wang *et al.,* [68] present a high-frequency FBG accelerometer without specifying its linear operating frequency and region.

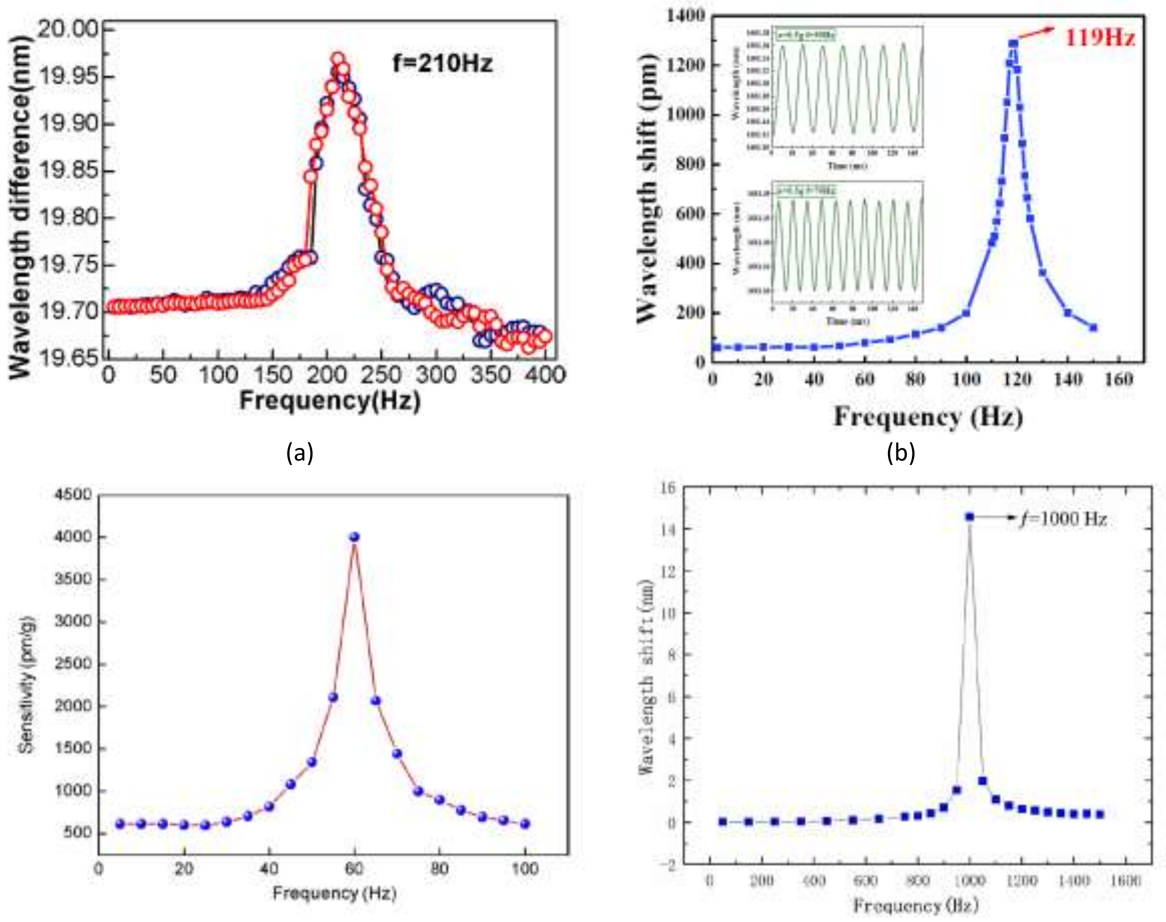

(a) (b)

(c) (d)

Fig. 15. Sensitivity/wavelength shift plots (a) [59] (b) [60] (c) [65] (d) [68]

Figures 16 depict an additional four studies, wherein researchers similarly employ single excitation frequencies at each time for exploring the wavelength shift response under constant acceleration while varying excitation frequencies. Qiu *et al.,* [69] introduced two different types of low-frequency FBG accelerometers, namely tilted and horizontal, subjecting them to testing within an excitation frequency range of 6 to 60 Hz with 2 Hz intervals. Remarkably, both accelerometer types exhibited a consistent pattern of wavelength shift characterized by linear increases, with linear operating frequency range is between 6 to 30 Hz (Figure 16(a)). Liu *et al.,* [72] conducted experiments on their FBG accelerometer within the frequency range of 5 to 60 Hz, using intervals of 5 Hz and an acceleration of 1 m/s². Their findings revealed a linear increase in wavelength shift concerning excitation frequencies specifically within the linear operating frequency of 5 to 20 Hz (Figure 16(b)). The studies conducted by Wei *et al.,* [73] and Luo *et al.,* [74] chose a large frequency interval of 50 Hz. This is due to the fact that their research focused on a high-frequency FBG accelerometer, which has a linear operating frequency range of 0 to 800 Hz (refer to Figure 16(c)) and 50 to 400 Hz (refer to Figure 16(d)), respectively.

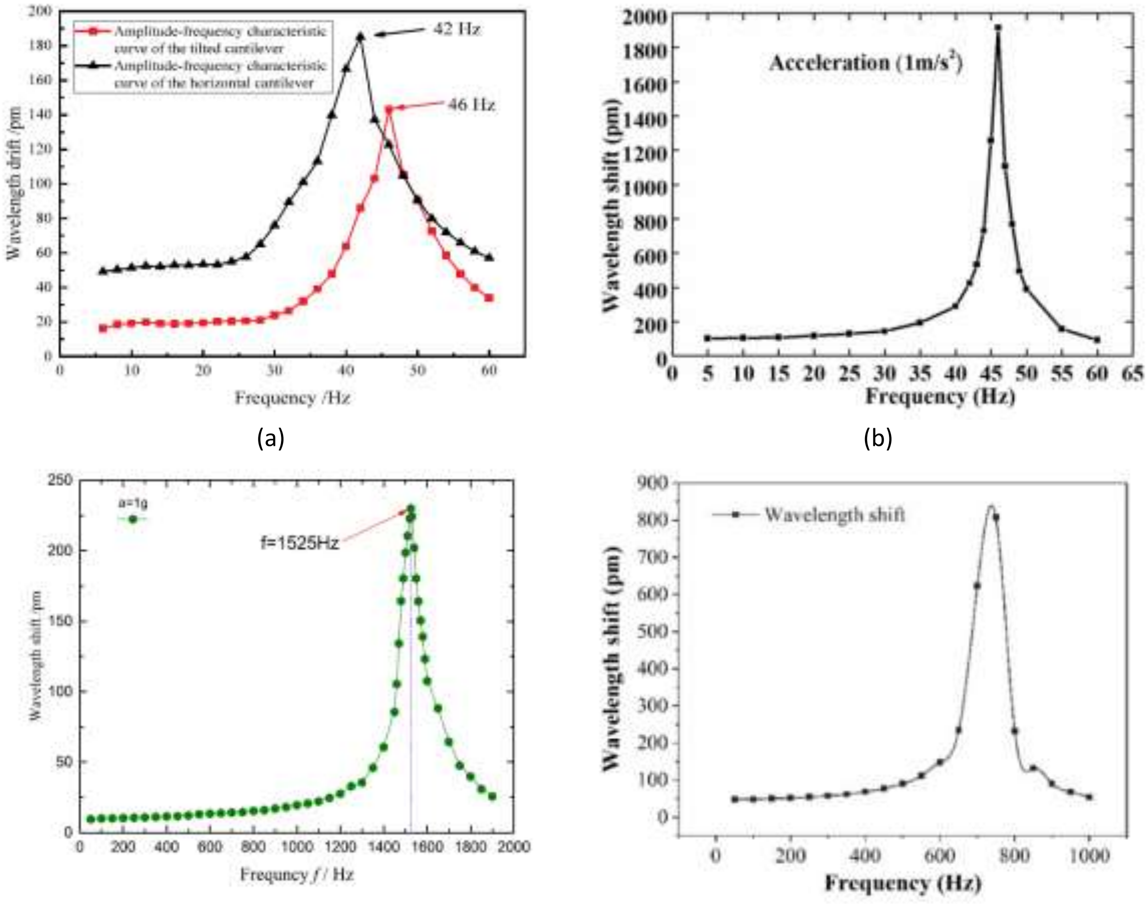

(a) (b)

(c) (d)

Fig. 16. Sensitivity/wavelength shift plots (a) [69] (b) [72] (c) [73] (d) [74]

This subsection reveals a prevalent trend among researchers, who predominantly conduct experiments using a single excitation frequency at a time rather than employing a swept excitation frequency method. Another noteworthy conclusion is that the linear operating frequency range determined through average or basic fitting typically falls below the resonant frequency, with some studies not adhering to the recommended guideline of at least one-half or one-third of the resonant frequency.

6. Sensitivity Enhancement of Cantilever FBG Accelerometer

FBG accelerometer generally exhibits an inverse relationship between its sensitivity and resonant frequency. Therefore, designing an FBG accelerometer involves a trade-off between sensitivity and resonant frequency [52,57]. To optimize both parameters require a careful design of the mechanical and optical components of the FBG accelerometer. Researchers strive to strike a balance between a broad frequency response and high sensitivity for accurate measurements in specific applications

Numerous studies have explored on sensitivity enhancement of cantilever FBG accelerometer and definitely these studies had included different designs that have their own frequency response range.

Li *et al.,* [56] conducted a study wherein they implemented a FBG accelerometer, utilizing the structural configuration of an equal-section cantilever beam along with the lever amplification principle as an integrated approach aimed at improving the response sensitivity of the accelerometer. With a resonant frequency of 171.5 Hz, the accelerometer exhibits a robust response to low-frequency acceleration excitation signals ranging from 5 Hz to 90 Hz and its sensitivity in the working direction is measured at 239.12 pm/g. Pursuing a similar goal, Jiang *et al.,* [60] presented a FBG accelerometer wherein the effective length of the optical fibre was reduced by altering the base of the accelerometer. As a result, the FBG accelerometer exhibits a higher resonant frequency of 119 Hz, accompanied by a sensitivity of 134.29 pm/g in the main direction (*z*-axis) within a flat region ranging from 2 to 60 Hz. Jiang *et al.,* [52] applied a bearing in the cantilever FBG accelerometer for the purposes to decrease energy loss during vibration and enhance sensitivity. The FBG accelerometer provides 111.02 Hz resonant frequency with linear response over abroad frequency range from 0.5Hz to 40Hz and successful to record a high sensitivity of 575.8 pm/g. Research done by Chen *et al.,* [75] proposed FBG accelerometers employing a short FBG inscribed in single-mode fibre (SMF) with cladding thickness significantly less than 125 µm. The FBG accelerometer that fabricated within a 50-µm cladding-diameter fibre, was selected for demonstrating sensitivity enhancement and it exhibits a linear response of approximately 2150±30 pm/g across a frequency range from 0.5 Hz to 30 Hz, with the accelerometer's resonant frequency measuring about 63 Hz. A study done by Parida *et al.,* [76] revealed that a sensitivity of 821 pm/g is attained, coupled with a natural frequency of 64 Hz. This achievement is achieved through a novel T-shaped cantilever-based mechanical sensor head, wherein two FBG sensors are integrated in a differential sensing configuration. Next with the same aim of researchers abovementioned and has concept similarity with Parida *et al.,* [57,76], presented a novel double-L cantilever-based FBG accelerometer. High sensitivity of 406.7 pm/g is demonstrated with a natural frequency of 86 Hz and operating frequency range from 5 Hz to 50 Hz. On the other hand, Angel *et al.,* [38] proposed more simpler structure in enhancing the sensitivity of the cantilever FBG accelerometer. A section of the fibre that contains the FBG is positioned perpendicularly to the surface of the cantilever, located between the tip of the cantilever and the frame of the sensor. This study indicates a sensitivity of 330 pm/g and a natural frequency of 227.3 Hz. With some modification of position and location of the FBGs on the accelerometer structure [66], later successful to enhance the sensitivity of the accelerometer to 339 pm/g and the same natural frequency is similar with previous research. Li *et al.,* [77] developed an FBG transducer with a low resonant frequency of 34 Hz for micro-vibration measurement. The micro-vibration sensor in this study is designed by directly treating the optical fibre as an elastomer and incorporating two FBG sensors. The mass is securely affixed at the midpoint of the fibre and the vertical vibration of the mass is transformed into axial tension/compression of the fibre. The experiment conclusion shows that the sensor sensitivity is 2362 pm/g within the range of 200–1200 mm/s^2. Several interesting FBG accelerometers have achieved a medium operating frequency and the medium operating frequency is apparent from a variety of designs and approaches. Li *et al.,* [78] have proposed a sensitization process method for a pasted FBG cantilever beam accelerometer to increase the resonant frequency with its design and as a result it is able to reach the working band from 0 to 150 Hz with the resonant frequency of 200 Hz. Furthermore, with a 1mm separation between the fibre core and the cantilever beam, the sensor's sensitivity is enhanced by 2.9 times compared to the conventional process.

In cantilever FBG accelerometers, incorporating a tip mass is widely recognized as one of the most effective methods [39,40,42,43,45,63,64] (refer to Table 4 for a tabular overview of cantilever FBG accelerometers with tip mass and their sensitivity for recent development). Gagliardi *et al.,* [42] employed a tip mass in combination with laser-based interrogation techniques to enhance sensitivity and broaden the frequency range. However, the reported information did not include a specific sensitivity value. Basumallick *et al.,* [40,63] explored the incorporation of a tip mass to enhance sensitivity by adjusting the effective distance between the sensor axis and the neutral axis of the cantilever. Their investigation resulted in achieving a sensitivity of 450 pm/g. Conversely, it is noteworthy to highlight that FBG accelerometers featuring elastic diaphragms have demonstrated elevated sensitivity and fundamental frequency. These devices are frequently equipped with either a single diaphragm [32] or double diaphragms [31,79-81]. Furthermore, Liu *et al.,* [31,81] demonstrated that double-point encapsulation enhances the sensitivity of FBG accelerometers. Additionally, double-point encapsulation proves effective in mitigating issues such as FBG chirp, spectrum splitting and inefficient wavelength detection. Furthermore, a hybrid design involving a cantilever beam and a single diaphragm has been proposed, achieving an exceptionally high sensitivity of approximately 100 pm/g. [82].

Table 4
Summary of sensitivity and resonant frequency for recent cantilever FBG accelerometer with tip mass

Reference	Technique	Sensitivity	Resonant frequency
[56]	Equal-section cantilever beam in combination with the lever amplification principle	239.12 pm/g	171.5 Hz
[60]	Changing the base of cantilever FBG accelerometer	134.29 pm/g	119 Hz
[52]	FBG Accelerometer Based on a Bearing	575.8pm/g	111.02 Hz
[75]	Thin-Cladding FBG	2150±30 pm/g	63 Hz
[76]	T-shaped rigid cantilever beam, a thin leaf spring and a proof mass	821 pm/g of	64 Hz
[57]	Double-L Cantilever Based FBG Accelerometer	406.7 pm/g	86 Hz
[38]	FBG perpendicular to the cantilever surface	330 pm/g	227.3 Hz
[66]	FBG in-line with the vertical axis	339 pm/g	227.3 Hz
[39]	Distance between the axis of the FBG sensor to the neutral axis of the cantilever.	~1062 pm/g	18.75 Hz
[77]	Micro-vibration sensor (possesses two FBGs)	2362 pm/g	34 Hz
[78]	Pasted FBG-based cantilever beam accelerometer’s sensitization process model	9.1 pm/g	200 Hz
[82]	Two L-shaped rigid cantilever beams	100 pm/g	170 Hz
[70]	A single cantilever with a tip mass	8.63 – 11.77 pm/g (5 to 25 Hz excitation frequencies)	48.9 Hz

7. Sensitivity Characteristic of Cantilever FBG Accelerometer

For FBG accelerometers, regardless the structural mechanisms employed, it is reasonable to assume that sensitivity remains linear within a specified range, which is one-third (33%) or one-half (50%) of the resonant frequencies [72,83-85]. For instance, Jiang *et al.,* [60] developed a FBG accelerometer that operates at a maximum frequency of 60 Hz (one-half), resonating at 119 Hz and exhibiting a sensitivity of 134.29 pm/g. Another study by Zhang *et al.,* [65] resulted in a FBG accelerometer with a maximum operating frequency of 25 Hz (42% - less than one-half), resonating at 60 Hz and featuring a sensitivity of 1296 pm/g. Similarly, Wang *et al.,* [86] created a FBG accelerometer with a maximum operating frequency of 1200 Hz (31% - less than one-third), resonating at 3806 Hz and demonstrating a sensitivity of 4.01 pm/g.

Nevertheless, many research studies are also capable of generating operating frequencies exceeding one-half of the resonant frequency, given that sensitivity was computed using basic fitting methods, even though the actual sensitivity plot might be non-linear or scattered. For instance, Parida *et al.,* [57] achieved a maximum operating frequency at 50 Hz (58% - more than one-half) with a resonance frequency at 86 Hz and a sensitivity of 406.7 pm/g. Li *et al.,* [56] reached a maximum operating frequency at 90 Hz (52% - more than one-half) with a resonance frequency at 171.5 Hz and a sensitivity of 239.12 pm/g. Additionally, Nguyen *et al.,* [50] attained a maximum operating frequency at 900 Hz (72% - more than one-half) with a resonance frequency at 1250 Hz and a sensitivity of 67.9 pm/g. Similarly, Hong *et al.,* [87], Wei *et al.,* [73], Fan *et al.,* [34], Jiang *et al.,* [52], Luo *et al.,* [74] and Qiu *et al.,* [69] achieved various maximum operating frequencies, all exceeding one-half of the respective resonance frequencies, with corresponding sensitivities.

The sensitivity of the FBG accelerometer can be determined through two methods, either by:

i. Predicting sensitivity using numerical data derived from the mathematical model of the FBG accelerometer or
ii. Identifying sensitivity through empirical data acquired from actual acceleration measurements.

Further literature, which will be discussed in this section and beyond, presents study results that demonstrate the sensitivity pattern and emphasise that, the wavelength shift response is inherently non-linear at different excitation frequencies for the same acceleration value. Li *et al.,* [84] introduced an ultra-compact FBG accelerometer, establishing its sensitivity at 244 pm/g through numerical data and 633 pm/g through empirical data. Numerical and empirical data are both generated under a forcing frequency of 5 Hz and a progressively increasing base acceleration. In contrast to Li *et al.,* [84], Liu *et al.,* [72] determined the sensitivity of the symmetrical bent spring plates FBG accelerometer by employing:

i. Numerical data at a single maximum base acceleration of 1 m/s^2 at two forcing frequencies of 5 and 10 Hz.
ii. Empirical data at varying maximum base accelerations ranging from 1 to 6 m/s^2 and forcing frequencies of 5, 10, 15 and 20 Hz (Figure 17).

The sensitivity, determined to be 1067 pm/g through numerical data, aligns closely with the empirical value obtained. Nevertheless, it's noteworthy that the sensitivity of the FBG accelerometer exhibits a slight increase with rising forcing frequencies, measuring 1067 pm/g at 5 Hz, 1084 pm/g at 10 Hz, 1126 pm/g at 15 Hz and 1166 pm/g at 20 Hz.

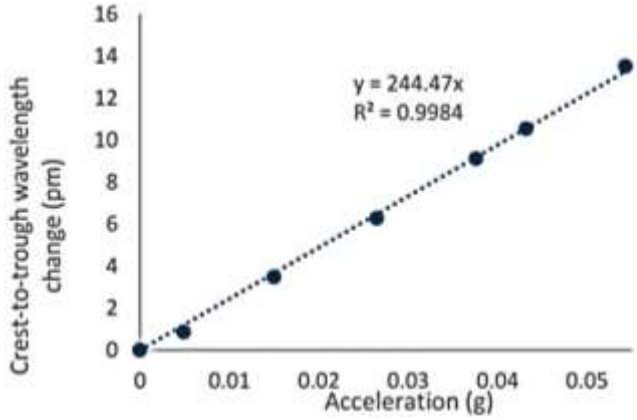

(a)

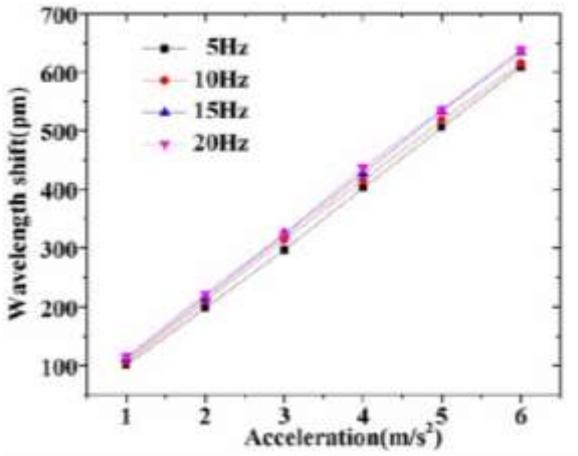

(b)

Fig. 17. Wavelength shift of the FBG accelerometer: (a) under different base acceleration at single excitation frequency of 5 Hz [84], (b) under different base accelerations and frequencies [72]

In addition, the results of another sensitivity analysis that was carried out by Li Wei *et al.,* [73] also demonstrate that the sensitivity is frequency-dependent. The novel miniatured FBG vibration sensor was put through a series of experiments with varying excitation frequencies ranging from 0 to 800 Hz. At 100 Hz excitation, the measured sensitivity was 9.8 pm/g. As the frequency increased, so did the sensitivity - reaching 11.43 pm/g at 300 Hz, 11.95 pm/g at 500 Hz, 12.77 pm/g at 600 Hz and topping out at 14.59 pm/g at the maximum tested frequency of 800 Hz (Figure 18(a)). Due to the fact that the percentage of sensitivity increment is less than 28%, the overall significance of the increment is not extremely large. Other research work by Luo *et al.,* [74] does not delve into the details of frequency dependency. Nonetheless, the sensitivity plot using experiment data (Figure 18(b)) clearly shows that the response of the wavelength shift FBG accelerometer is frequency dependent. To be more precise, the sensitivity is 49.89 pm/g at 100 Hz, 53.5 pm/g at 200 Hz, 60.9 pm/g at 300 Hz and 97.6 pm/g at 500 Hz. In line with similar findings in previous research [72,73], the sensitivity increases with increasing excitation frequencies. However, as the excitation frequencies increase, for example, at 500 Hz, the percentage increase in sensitivity is tremendous, over 100% greater than at 100 Hz.

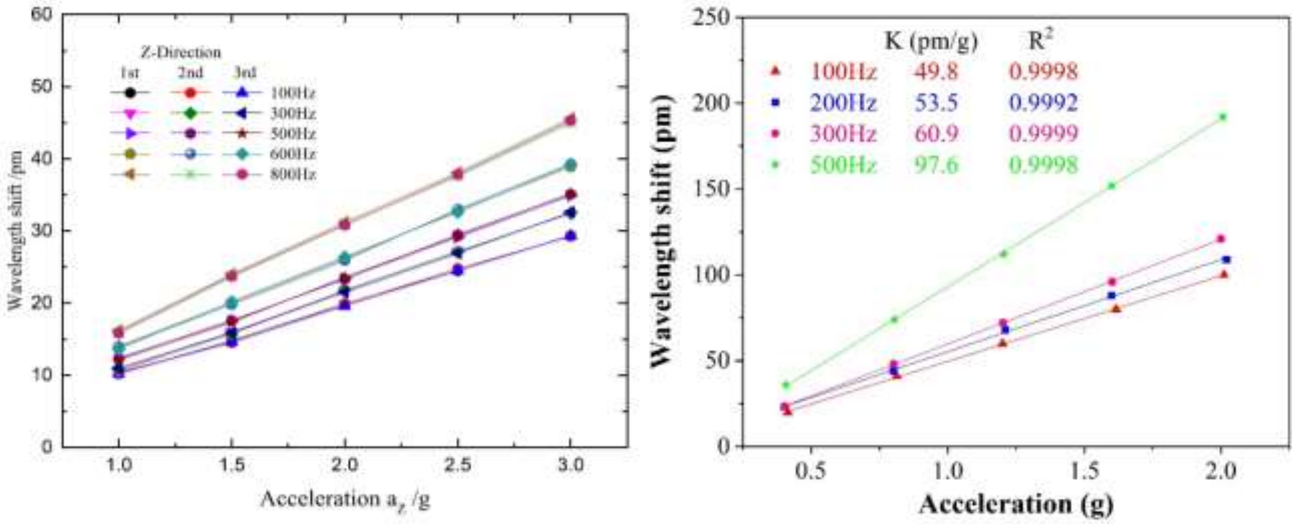

(a) (b)

Fig. 18. Wavelength shift of the FBG accelerometer under different base acceleration at excitation frequencies of (a) 100, 300, 500, 600 and 800 Hz [73] (b) 100, 200, 300 and 500 Hz [72]

The double-mass block FBG accelerometer, introduced by Wang, underwent a comprehensive experimental works under varying excitation frequencies at 50 Hz, 150 Hz and 250 Hz [68]. The acceleration ranged from 1 g to 4 g, with increments of 1 g at each excitation frequency. Although the frequency-dependent aspect was not covered in detail, the sensitivity plot (Figure 19(a)) makes it clearly evident that the FBG accelerometer is essentially frequency-dependent. Similar to Luo *et al.,* [74] excitation frequency likewise significantly increases the sensitivity. As evidenced by aforementioned studies by Wang *et al.,* [68], Wei *et al.,* [73] and Luo *et al.,* [74], the sensitivity of FBG accelerometer is found to be frequency-dependent, especially in the context of intermediate-low frequency accelerometers. In contrast, a study by Jiang study focuses specifically on low frequencies, highlighting the frequency-dependent nature of the FBG accelerometer, which operates effectively below 60 Hz [52]. The sensitivity, as depicted in Figure 19(b), displays variations within the low-frequency range, with small changes observed as the excitation frequency varies (about 5% different between 60 and 60 Hz). However, this observation does not change the fact that, in alignment with other research findings [68,73,74], the wavelength shifts response remains frequency-dependent, even in the context of low-frequency FBG accelerometers. Another study by Li *et al.,* [56], focusing on also low frequency FBG accelerometer with excitation frequencies falling within a similar range as Jiang *et al.,* [52], from 10 to 70 Hz, similarly indicates slight changes in sensitivity (Figure 19(c)). The observed difference in sensitivity between excitation frequencies at 70 Hz and 10 Hz is approximately 7%, aligning with the findings from the study conducted by Jiang *et al.,* [52].

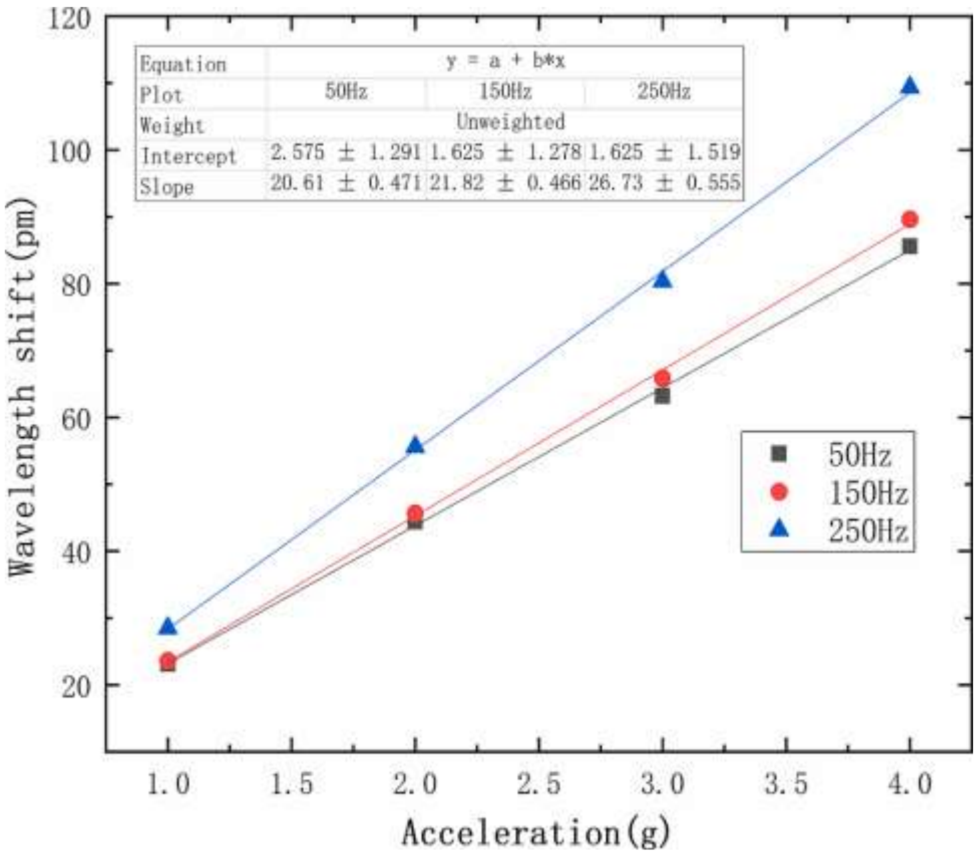
Equation
y = a + b*x
Plot
50Hz
150Hz
250Hz
Weight
Unweighted
Intercept
2.575 ± 1.291
1.625 ± 1.278
1.625 ± 1.519
Slope
20.61 ± 0.471
21.82 ± 0.466
26.73 ± 0.555
50Hz
150Hz
250Hz
Wavelength shift (pm)
Acceleration (g)
20
40
60
80
100
120
1.0
1.5
2.0
2.5
3.0
3.5
4.0

(a)

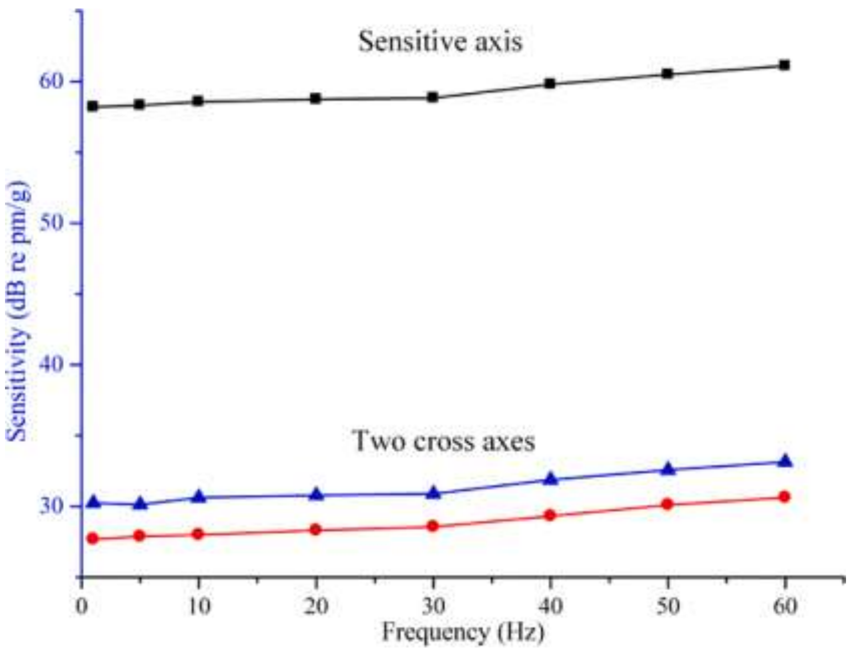
Sensitive axis
Two cross axes
Sensitivity (dB re pm/g)
Frequency (Hz)
30
40
50
60
0
10
20
30
40
50
60

(b)

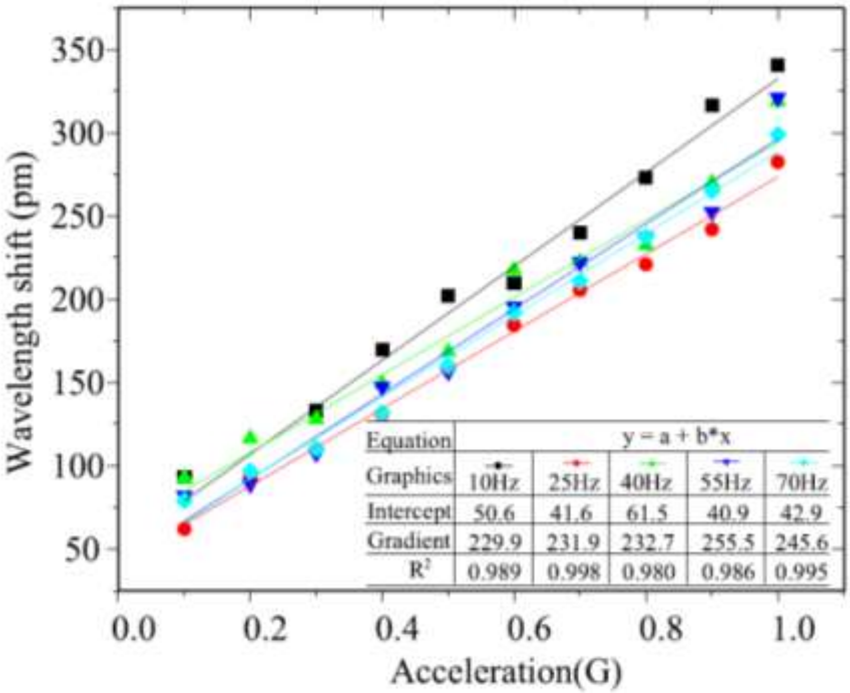

(c)

Fig. 19. Wavelength shift of the FBG accelerometer under different base acceleration at an excitation frequency of (a) 50, 150 and 250 Hz [68] (b) 1, 5, 10, 20, 30, 40, 50 and 60 Hz [52] (c) 10, 25, 40, 50, 70 Hz [52]

The sensitivity of the low-frequency FBG accelerometer obtained by Fan *et al.,* [34] exhibits a different characteristic. In contrast to other studies [52,68,73,74] in which the sensitivity increases with the frequency of the excitation, within the range of 5 to 60 Hz, the sensitivity exhibits a fluctuation that is approximately between 450 and 625 pm/g (Figure 20(a)). In the case of medium-high FBG accelerometers, a study conducted by Nguyen *et al.,* [50] indicates that the sensitivity increases as the excitation frequency increases. Consistent with the findings by Luo *et al.,* [74], it is observed that at high excitation frequencies, sensitivity experiences a substantial increase, reaching up to a 32% difference between excitation frequencies at 900 Hz and 500 Hz (Figure 20(b)).

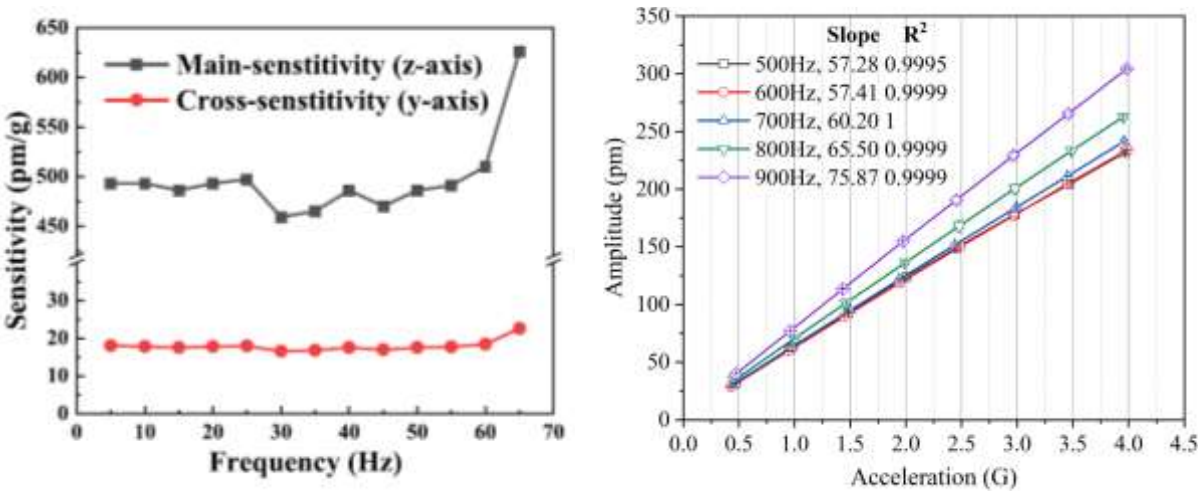

(a) (b)

Fig. 20. Wavelength shift of the FBG accelerometer under different base acceleration at an excitation frequency of (a) 5 - 60 Hz [34] (b) 500, 600, 700, 800 and 900 Hz [50]

All the works explained in this subsection, has proven regardless the design and mechanism as well as operating frequencies of the cantilever FBG accelerometers, the wavelength shift response is basically varied as the excitation frequency varies. Having different sensitivity for different excitation frequencies, impossible for the FBG accelerometer to be used for real measurement since the measured frequencies is unknown beforehand. In comparison to the majority of typical analogue voltage/electrical-charge accelerometers, the sensitivity of this accelerometer remains relatively constant over a broad frequency spectrum, as depicted in Figure 21, sourced from a renowned vibration tool manufacturer [88].

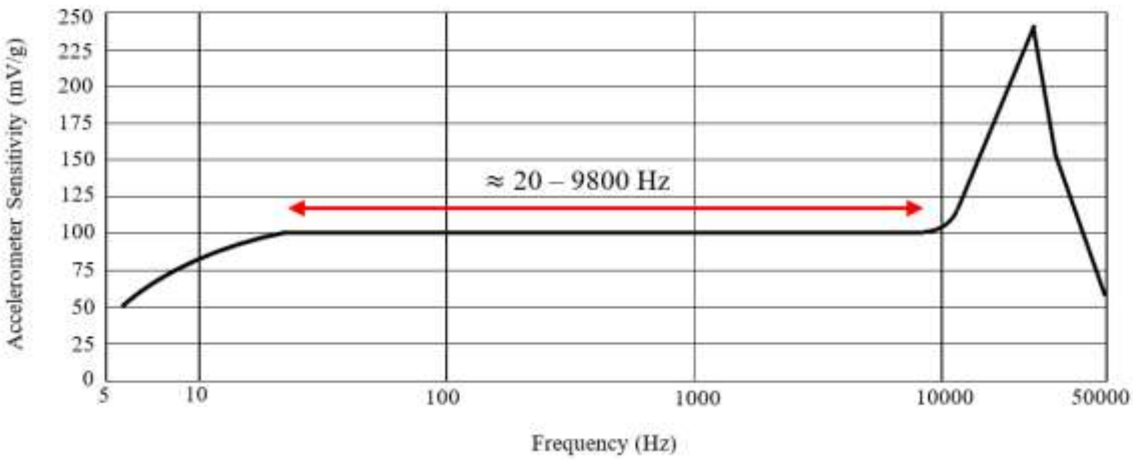

Fig. 21. Accelerometer sensitivity (mV/g) for analogue voltage/electrical-charge accelerometer [88]

There is not that many published evidence to support up the following claims about why the FBG sensor behaves nonlinearly, but here are a few:

i. Material Properties: The material properties of the fibre optic grating, including the type of material used (e.g., dopant concentration), fibre designs and the fabrication process, can contribute to nonlinearity [89].
ii. Installation Effects: The technique in which an FBG sensor is placed or glued to a structure might have an impact on its response (e.g., fully and double-points encapsulation). Nonlinearity might be caused by nonuniform strain distribution or installation issues [90].
iii. Host/structure to host the FBG sensor: In applications where FBG sensors are embedded in complex structures (basically, FBG sensors require mechanical hosts), the strain generated is proportional to the structural geometry of the host's behaviour, which might be linear or nonlinear [91].

Further support for the claim that the sensitivity of the FBG accelerometer is essentially frequency-dependent comes from observations made with a commercial FBG accelerometer (Figure 22). The calibration data, which spans 5.01 to 50.06 Hz, shows a sensitivity that is between 160.361 and 195.297 pm/ms^2 (1,573.14 and 1915.86 pm/g). This clear sensitivity difference within the specified frequency range indicates that measurements made even inside this calibrated region can introduce errors, which could affect the measurements' accuracy and precision.

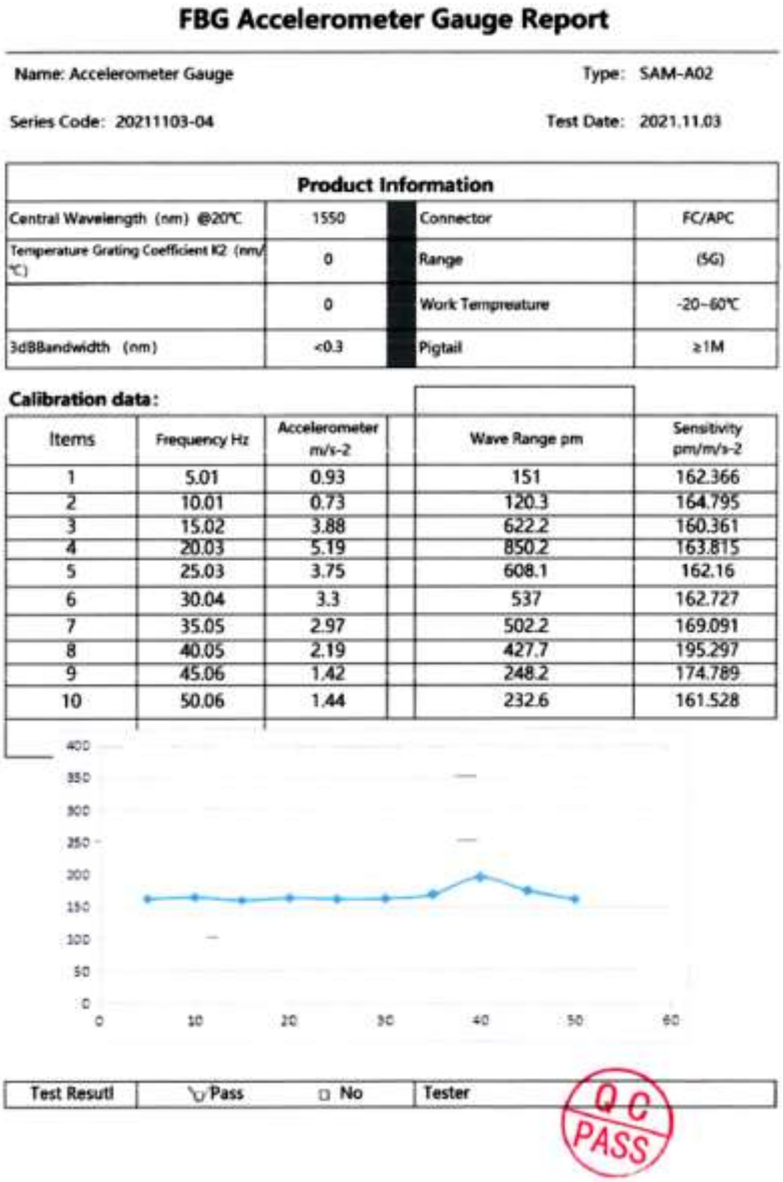

FBG Accelerometer Gauge Report

Name: Accelerometer Gauge Type: SAM-A02

Series Code: 20211103-04 Test Date: 2021.11.03

Product Information				
Central Wavelength (nm) @20℃	1550		Connector	FC/APC
Temperature Grating Coefficient K2 (nm/℃)	0		Range	(5G)
	0		Work Tempreature	-20~60℃
3dBBandwidth (nm)	<0.3		Pigtail	≥1M

Calibration data:

Items	Frequency Hz	Accelerometer m/s-2		Wave Range pm	Sensitivity pm/m/s-2
1	5.01	0.93		151	162.366
2	10.01	0.73		120.3	164.795
3	15.02	3.88		622.2	160.361
4	20.03	5.19		850.2	163.815
5	25.03	3.75		608.1	162.16
6	30.04	3.3		537	162.727
7	35.05	2.97		502.2	169.091
8	40.05	2.19		427.7	195.297
9	45.06	1.42		248.2	174.789
10	50.06	1.44		232.6	161.528

Test Resutl	√ Pass	□ No	Tester

Q C PASS

Fig. 22. Datasheet of commercialised FBG accelerometer

8. Research Gaps on Cantilever Beam Model and Sensitivity Studies of FBG Accelerometer

With regard to section 4, it is apparent that the model employed in all cantilever FBG accelerometers lacks consideration for crucial factors such as rotational inertia and shear force. The SDOF model, which is the simplest model, is commonly applied in most research involving cantilever FBG accelerometers. The simplicity of the SDOF model makes it a convenient dynamic model for gaining insights into the fundamental principles of cantilever FBG accelerometers. However, it is important to note that the SDOF model represents a significant simplification and may not fully capture the actual dynamics of a cantilever FBG accelerometer.

A widely used model for describing the behaviour of cantilever beams is the Timoshenko beam model. Notably, the rotational inertia and shear force are taken into account in the Timoshenko beam model [92]. This model has been employed in numerous disciplines of studies with a focus on precision, notably in applications such as cantilevered piezoelectric energy harvesters [93], robotic [94], building [95] and biomechanics [96]. However, it is worth noting that rotational inertia and shear force can be neglected, as is the case with the Euler-Bernoulli model, under specific conditions:

i. Excitation frequency within low range.
ii. Length to thickness ratio of the beam (*l/d*) was more than 20.

Since the Euler-Bernoulli model neglects shear deformation, the cross-sections of the beam are assumed to stay perpendicular to the deformed axis, as illustrated in Figure 23. Consequently, for a thick beam, the Timoshenko beam model gives small amount of shear forces (resulting in small shear deformation) and in such cases, the negligible effect of shear force, as assumed by the Euler-Bernoulli model, is valid. Meeting its criteria of low frequency and a thick beam, this model has been introduced by Khalid *et al.,* [70,71].

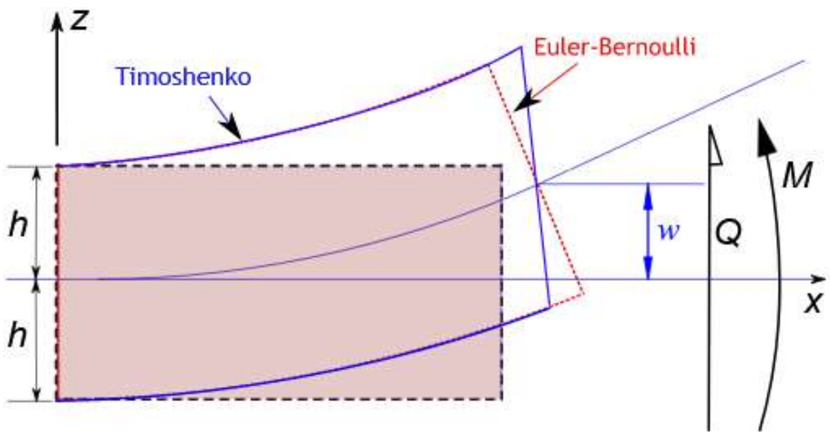

Fig. 23. Shear deformation of a Timoshenko beam model (blue) compared with that of a Euler Bernoulli beam model (red)

In addition to the Timoshenko and Euler-Bernoulli beam models, there are several other beam models, including Reddy-Bickford, Vlasov, Shear Deformable and Nonlinear beam models. The Reddy-Bickford beam model is derived for use in very short and thick beams, approximately *l/d* ≤ 1. This model accounts for the warping phenomenon, wherein the cross-sectional deformation in a bent beam is not constant. Therefore, the Reddy-Bickford beam model introduced higher-order shear distribution instead of a first-order shear theory [97]. In addition to accounting for shear deformation like the Timoshenko beam model, the Vlasov beam model incorporates axial deformation while neglecting consideration of rotational inertia [98]. This beam model is well-suited for the analysis of thin cantilever beams, where the walls are thin compared to the overall dimensions of the beam. On the other hand, the Shear Deformable beam model refers to any model that takes shear deformation into account in beam analysis, with the Timoshenko Beam Model is limited to its particular equations, assumptions and formulations. Nonlinear beam models, encompass a broader range of behaviours, going beyond the linear elastic assumptions of Euler-Bernoulli and Timoshenko models. Nonlinear beam models can account for large displacements, material nonlinearity and geometric nonlinearity. These models are applicable when beams undergo significant deformations, material properties change nonlinearly or the beam response becomes inherently nonlinear.

In terms of sensitivity, it has been demonstrated that sensitivity is frequency-dependent, a conclusion substantiated by experimental plots illustrating wavelength shift versus acceleration at different excitation frequencies, as in section 5. This conclusion finds support in the work of Basumallick *et al.,* [40] as articulated in their publication, where they state “*there is a frequency dependence of sensitivity as operating frequency is increased”*. As discussed earlier, the frequency-dependent of FBG accelerometer can result from factors such as material properties, installation effects and the host structure's behaviour when FBG sensors embedded in complex structures. This claim also holds merit because, if the system is modelled using a more precise model, such as Euler-Bernoulli or Timoshenko models, taking into account multiple modes of vibrations, it results in frequency-dependent effects. The use of averaging and basic fitting to approximate the sensitivity of the cantilever FBG accelerometer, as demonstrated in studies such as Fan *et al.,* [34], Jiang *et al.,* [52], Wei *et al.,* [73] and Hong *et al.,* [87], however, will lead to inaccuracies. The frequency-dependent concern is further validated by industry support, given that the sensitivity varies at different excitation frequencies, as outlined in the manufacturer's datasheet (Figure 22). This variability is problematic since the excitation frequencies are unknown before conducting acceleration measurements. It is suggested that the frequency-dependent issue can be resolved by implementing a neural network or machine learning as an "identifier black-box" as has been initially done by Hassan *et al.,* [99] and Khalid *et al.,* [100].

Acknowledgement
The author(s) disclosed receipt of the following financial support for the research, authorship and/or publication of this article: Universiti Malaysia Pahang Al-Sultan Abdullah for their financial support through RDU240304 grant scheme. Data related to the research presented in this manuscript shall be made available through the University Malaysia Pahang Al-Sultan Abdullah's Institutional Repository.

References
[1] Bates, Regis J. *Optical switching and networking handbook*. McGraw-Hill Professional, 2001.
[2] Holzmann, Gerard J. and Björn Pehrson. *The early history of data networks*. IEEE Computer Society Press, 1995.
[3] Hecht, Jeff. *City of light: the story of fiber optics*. Oxford university press, 2004.
[4] Hansell, Clarence W. "Picture transmission." U.S. Patent 1,751,584, issued March 25, 1930.
[5] Kapron, Felix P., Donald B. Keck and Robert D. Maurer. "Radiation losses in glass optical waveguides." *Applied Physics Letters* 17, no. 10 (1970): 423-425. https://doi.org/10.1063/1.1653255
[6] Lee, Byoungho. "Review of the present status of optical fiber sensors." *Optical fiber technology* 9, no. 2 (2003): 57-79. https://doi.org/10.1016/S1068-5200(02)00527-8
[7] Mihailov, Stephen J. "Fiber Bragg grating sensors for harsh environments." *Sensors* 12, no. 2 (2012): 1898-1918. https://doi.org/10.3390/s120201898
[8] Bragg, William Henry and William Lawrence Bragg. "The reflection of X-rays by crystals." *Proceedings of the Royal Society of London. Series A, Containing Papers of a Mathematical and Physical Character* 88, no. 605 (1913): 428-438. https://doi.org/10.1098/rspa.1913.0040
[9] Hill, Kenneth O., Yoshihisa Fujii, Derwyn C. Johnson and Brian S. Kawasaki. "Photosensitivity in optical fiber waveguides: Application to reflection filter fabrication." *Applied physics letters* 32, no. 10 (1978): 647-647. https://doi.org/10.1063/1.89881
[10] Hill, Kenneth O. and Gerald Meltz. "Fiber Bragg grating technology fundamentals and overview." *Journal of lightwave technology* 15, no. 8 (1997): 1263-1276. https://doi.org/10.1109/50.618320
[11] Morey, W. W., G. Meltz and W. H. Glenn. "Holographically generated gratings in optical fibers." *Optics and Photonics News* 1, no. 7 (1990): 14-16. https://doi.org/10.1364/OPN.1.7.000014
[12] Hill, K. O., B. Malo, K. A. Vineberg, F. Bilodeau, D. C. Johnson and I. Skinner. "Efficient mode conversion in telecommunication fibre using externally written gratings." *Electronics letters* 26, no. 16 (1990): 1270-1272. https://doi.org/10.1049/el:19900818
[13] Mita, Akira and Isamu Yokoi. "Fiber Bragg grating accelerometer for structural health monitoring." In *Fifth international conference on motion and vibration control (MOVIC 2000), Sydney, Australia*. 2000.
[14] Meltz, Gerald, William W. Morey and William H. Glenn. "Formation of Bragg gratings in optical fibers by a transverse holographic method." *Optics letters* 14, no. 15 (1989): 823-825. https://doi.org/10.1364/OL.14.000823
[15] Malo, B., Kenneth O. Hill, F. Bilodeau, D. C. Johnson and Jacques Albert. "Point-by-point fabrication of micro-Bragg gratings in photosensitive fibre using single excimer pulse refractive index modification techniques." *Electronics Letters* 29, no. 18 (1993): 1668-1669. https://doi.org/10.1049/el:19931110
[16] Hill, K., F. O. Bilodeau, D. C. Johnson and Jacques Albert. "Bragg gratings fabricated in monomode by UV exposure through a phase mask photosensitive optical fiber." *Applied Physics Letters* 62, no. 10 (1993). https://doi.org/10.1063/1.108786

[17] Tahir, Bashir Ahmed, Jalil Ali and Rosly Abdul Rahman. "Fabrication of fiber grating by phase mask and its sensing application." *Journal of optoelectronics and advanced materials* 8, no. 4 (2006): 1604.
[18] Chen, Jinjie, Bo Liu and Hao Zhang. "Review of fiber Bragg grating sensor technology." *Frontiers of Optoelectronics in China* 4 (2011): 204-212. https://doi.org/10.1007/s12200-011-0130-4
[19] Majumder, Mousumi, Tarun Kumar Gangopadhyay, Ashim Kumar Chakraborty, Kamal Dasgupta and Dipak Kumar Bhattacharya. "Fibre Bragg gratings in structural health monitoring—Present status and applications." *Sensors and Actuators A: Physical* 147, no. 1 (2008): 150-164. https://doi.org/10.1016/j.sna.2008.04.008
[20] Naguib, Bassem Adel, Mohamed Maher Ata, Mahmoud M. Alzalabani and Bedir B. Yousif. "Performance evaluation and enhancement of apodized fiber Bragg grating for dispersion compensation." *AIP Advances* 11, no. 1 (2021). https://doi.org/10.1063/5.0026190
[21] Canning, John. "Fibre gratings and devices for sensors and lasers." *Laser & Photonics Reviews* 2, no. 4 (2008): 275-289. https://doi.org/10.1002/lpor.200810010
[22] Raghuwanshi, Sanjeev Kumar and Akash Srivastav. "Review of microwave photonics technique to generate the microwave signal by using photonics technology." *Journal of Optical Communications* 39, no. 1 (2017): 25-35. https://doi.org/10.1515/joc-2016-0046
[23] Liu, Qinpeng, Xue He, Xueguang Qiao, Tong Sun and Kenneth TV Grattan. "Design and modeling of a high sensitivity fiber Bragg grating-based accelerometer." *IEEE Sensors Journal* 19, no. 14 (2019): 5439-5445. https://doi.org/10.1109/JSEN.2019.2904218
[24] Muhamad Shukri, Nur Ainaa Adhreena, Zohari, Mohd Hafizi and Vorathin, E. "Surface Strain Measurement on Pressurized Thick-Walled Pipe by Fiber Bragg Grating Sensor and Strain Gauges," *Journal of Advanced Research in Fluid Mechanics and Thermal Sciences, vol. 84,* no. 2, (2021): 1-9.
[25] Todd, M. D., G. A. Johnson, B. A. Althouse and S. T. Vohra. "Flexural beam-based fiber Bragg grating accelerometers." *IEEE Photonics Technology Letters* 10, no. 11 (1998): 1605-1607. https://doi.org/10.1109/68.726764
[26] Guo, Yongxing, Min Chen, Li Xiong, Xinglin Zhou and Cong Li. "Fiber Bragg grating based acceleration sensors: A review." *Sensor Review* 41, no. 1 (2021): 101-122. https://doi.org/10.1108/SR-10-2020-0243
[27] Li, Shili, Benli Yu, Xuqiang Wu, Jinhui Shi, Qiang Ge, Gang Zhang, Mengzhen Guo, Yifan Zhang, ShaSha Fang and Cheng Zuo. "Low-cost fiber optic extrinsic Fabry–Perot interferometer based on a polyethylene diaphragm for vibration detection." *Optics Communications* 457 (2020): 124332. https://doi.org/10.1016/j.optcom.2019.124332
[28] Wang, Zhaogang, Wentao Zhang, Jing Han, Wenzhu Huang and Fang Li. "Diaphragm-based fiber optic Fabry–Perot accelerometer with high consistency." *Journal of Lightwave Technology* 32, no. 24 (2014): 4810-4815. https://doi.org/10.1109/JLT.2014.2367001
[29] Li, Shili, Xuqiang Wu, Jinhui Shi, Qiang Ge, Gang Zhang and Benli Yu. "Fabry-Perot interferometer based on an aluminum-polyimide composite diaphragm integrated with mass for acceleration sensing." *Ieee Access* 7 (2019): 186510-186516. https://doi.org/10.1109/ACCESS.2019.2960797
[30] Li, Ruiya, Yuegang Tan, Junjun Bing, Tianliang Li, Liu Hong, Junwei Yan, Jianmin Hu and Zude Zhou. "A diaphragm-type highly sensitive fiber Bragg grating force transducer with temperature compensation." *IEEE Sensors Journal* 18, no. 3 (2017): 1073-1080. https://doi.org/10.1109/JSEN.2017.2779853
[31] Liu, Qinpeng, Xueguang Qiao, Zhen'an Jia, Haiwei Fu, Hong Gao and Dakuan Yu. "Large frequency range and high sensitivity fiber Bragg grating accelerometer based on double diaphragms." *IEEE Sensors Journal* 14, no. 5 (2014): 1499-1504. https://doi.org/10.1109/JSEN.2013.2296932
[32] Liu, Qin Peng, Xue Guang Qiao, Jan Lin Zhao, Zhen An Jia, Hong Gao and Min Shao. "Novel fiber Bragg grating accelerometer based on diaphragm." *IEEE Sensors Journal* 12, no. 10 (2012): 3000-3004. https://doi.org/10.1109/JSEN.2012.2201464
[33] Liu, Qinpeng, Wangfei Liu, Chunfang Wang, Rong Zhang, Wei Fan, Dakuan Yu and Xueguang Qiao. "High figure of merit and low cross sensitivity fiber Bragg grating accelerometer based on double grid-diaphragms." *IEEE Sensors Journal* 21, no. 24 (2021): 27503-27509. https://doi.org/10.1109/JSEN.2021.3124030
[34] Fan, Wei, Jin Wen, Hong Gao and Xueguang Qiao. "Low-frequency fiber Bragg grating accelerometer based on diaphragm-type cantilever." *Optical Fiber Technology* 70 (2022): 102888. https://doi.org/10.1016/j.yofte.2022.102888
[35] Zhang, Faxiang, Shaodong Jiang, Chang Wang, Jiasheng Ni and Qingchao Zhao. "Broadband and high sensitivity FBG accelerometer based on double diaphragms and h-shaped hinges." *IEEE sensors journal* 21, no. 1 (2020): 353-359. https://doi.org/10.1109/JSEN.2020.3013611
[36] Rahim, Muhammad Rais, MD Mofazzal Hossain and Mohd Firdaus Hassan. "Development and comprehensive investigation of a lightweight FBG accelerometer for small structure acceleration measurements." *Measurement Science and Technology* 35, no. 10 (2024): 105106. https://doi.org/10.1088/1361-6501/ad5dea

[37] Reghuprasad, Aarathy Ezhuthupally, Chiara Colombero and Alberto Godio. "Serially connected cantilever beam-based FBG accelerometers: design, optimization and testing." *Sensors* 23, no. 6 (2023): 3188. https://doi.org/10.3390/s23063188

[38] Angel, Casas-Ramos Miguel and Sandoval-Romero Gabriel Eduardo. "Uniaxial fiber Bragg grating accelerometer: Enhanced sensitivity and bandwidth." In *2015 Photonics North*, pp. 1-1. IEEE, 2015. https://doi.org/10.1109/PN.2015.7292509

[39] Basumallick, Nandini, Palas Biswas, Kamal Dasgupta and Somnath Bandyopadhyay. "Design optimization of fiber Bragg grating accelerometer for maximum sensitivity." *Sensors and Actuators A: Physical* 194 (2013): 31-39. https://doi.org/10.1016/j.sna.2013.01.039

[40] Basumallick, Nandini, I. Chatterjee, P. Biswas, Kamal Dasgupta and S. Bandyopadhyay. "Fiber Bragg grating accelerometer with enhanced sensitivity." *Sensors and Actuators A: Physical* 173, no. 1 (2012): 108-115. https://doi.org/10.1016/j.sna.2011.10.026

[41] Zhang, Jian, Yanling Xiong and Aihuan Yang. "Study of FBG application in acceleration sensing." In *2009 IEEE 9th International Conference on the Properties and Applications of Dielectric Materials*, pp. 1106-1109. IEEE, 2009. https://doi.org/10.1109/ICPADM.2009.5252306

[42] Gagliardi, G., M. Salza, P. Ferraro, P. De Natale, A. Di Maio, S. Carlino, G. De Natale and Enzo Boschi. "Design and test of a laser-based optical-fiber Bragg-grating accelerometer for seismic applications." *Measurement Science and Technology* 19, no. 8 (2008): 085306. https://doi.org/10.1088/0957-0233/19/8/085306

[43] Zhu, Yinian, Ping Shum, Chao Lu, Beatrys M. Lacquet, Pieter L. Swart and Stephanus J. Spammer. "Fiber Bragg grating accelerometer with temperature insensitivity." *Microwave and Optical Technology Letters* 37, no. 2 (2003): 151-153. https://doi.org/10.1002/mop.10852

[44] Zhang, Yan, Sanguo Li, Zhifan Yin, Robert Pastore Jr, Kurt O'Donnell, Michael Pellicano, John Kosinski and Hong-Liang Cui. "Fiber Bragg grating sensors for seismic wave detection." In *17th International Conference on Optical Fibre Sensors*, vol. 5855, pp. 1008-1011. SPIE, 2005. https://doi.org/10.1117/12.623728

[45] Zhang, Wei-gang, Zhi-gang Wu, Yan-ge Liu, Yi-fei Yang, Gui-yun Kai, Qi-da Zhao, Shu-zhong Yuan et al. "Principles and realizations of FBG wavelength tuning with elastic beams." *Optoelectronics letters* 1 (2005): 5-9.

[46] Kalenik, Jerzy and Ryszard Pająk. "A cantilever optical-fiber accelerometer." *Sensors and Actuators A: Physical* 68, no. 1-3 (1998): 350-355. https://doi.org/10.1016/S0924-4247(98)00066-1

[47] Jia, Zhen'an, Xianfeng Zhao, Wei Fan, Hong Gao, Qinpeng Liu, Zhen Yong, Yinggang Liu and Kaiqing Yang. "A two-dimensional cantilever beam vibration sensor based on fiber Bragg Grating." *Optical Fiber Technology* 61 (2021): 102447. https://doi.org/10.1016/j.yofte.2020.102447

[48] Casas-Ramos, Miguel Angel and Gabriel Eduardo Sandoval-Romero. "Modified optical fiber Bragg grating accelerometer." In *2015 Argentine School of Micro-Nanoelectronics, Technology and Applications (EAMTA)*, pp. 28-32. IEEE, 2015. https://doi.org/10.1109/EAMTA.2015.7237374

[49] Li, Tianliang, Yuegang Tan, Zude Zhou and Qin Wei. "Pasted type distributed two-dimensional fiber Bragg grating vibration sensor." *Review of Scientific Instruments* 86, no. 7 (2015). https://doi.org/10.1063/1.4927456

[50] Nguyen, Thi Thuy-Vy, Hoang-Dang Le, Hsiang-Cheng Hsu, Chi-Ngon Nguyen and Chia-Chin Chiang. "A medium-high frequency FBG accelerometer based on a V-shaped flexible hinge." *Measurement* 224 (2024): 113865. https://doi.org/10.1016/j.measurement.2023.113865

[51] Qiu, Zhongchao, Kai Su, Jinquan Zhang, Rui Sun and Yuntian Teng. "A miniaturized low-frequency FBG accelerometer based on symmetrical cantilever beam." *IEEE Sensors Journal* 23, no. 6 (2023): 5831-5840. https://doi.org/10.1109/JSEN.2023.3241167

[52] Jiang, Shaodong, Yingying Wang, Faxiang Zhang, Zhihui Sun and Chang Wang. "A high-sensitivity FBG accelerometer and application for flow monitoring in oil wells." *Optical Fiber Technology* 74 (2022): 103128. https://doi.org/10.1016/j.yofte.2022.103128

[53] Wu, Hao, Qijing Lin, Na Zhao, Libo Zhao, Guoxi Luo and Zhuangde Jiang. "A high-frequency acceleration sensor based on fiber grating." *IEEE Transactions on Instrumentation and Measurement* 70 (2021): 1-8. https://doi.org/10.1109/TIM.2021.3073394

[54] Lim, Kok-Sing, Muhammad Khairol Annuar Zaini, Zhi-Chao Ong, Fairul Zahri Mohamad Abas, Muhammad Aizi Bin Mat Salim and Harith Ahmad. "Vibration mode analysis for a suspension bridge by using low-frequency cantilever-based FBG accelerometer array." *IEEE Transactions on Instrumentation and Measurement* 70 (2020): 1-8. https://doi.org/10.1109/TIM.2020.3018578

[55] Li, Shuangshuang, Zhongyao Feng, Qiqi Ma, Ruohui Wang, Rui Zhou and Xueguang Qiao. "Fiber Bragg grating accelerometer based on symmetrical tilting cantilever beams and solder glass packaging for harsh environment." *Optical Fiber Technology* 65 (2021): 102579. https://doi.org/10.1016/j.yofte.2021.102579

[56] Li, Huidong, Xuan Zhang, Rui Zhou and Xueguang Qiao. "Low frequency fiber optic accelerometer based on lever amplification structure." *Optical Fiber Technology* 80 (2023): 103434. https://doi.org/10.1016/j.yofte.2023.103434

[57] Parida, Om Prakash, Jineesh Thomas, Jagannath Nayak and Sundarrajan Asokan. "Double-L cantilever-based fiber Bragg grating accelerometer." *IEEE Sensors Journal* 19, no. 23 (2019): 11247-11254. https://doi.org/10.1109/JSEN.2019.2936463

[58] Yang, Shuang, Jun Li, Yuquan Tang, Miao Sun, Gang Gao, Xu'an Liu, Bo Shi and Fengzhong Dong. "Analysis of the performance of strain magnification using uniform rectangular cantilever beam with fiber Bragg gratings." *Sensors and Actuators A: Physical* 273 (2018): 266-275. https://doi.org/10.1016/j.sna.2018.01.017

[59] Feng, Dingyi, Xueguang Qiao, Hangzhou Yang, Qiangzhou Rong, Ruohui Wang, Yanying Du, Manli Hu and Zhongyao Feng. "A fiber Bragg grating accelerometer based on a hybridization of cantilever beam." *IEEE Sensors Journal* 15, no. 3 (2014): 1532-1537. https://doi.org/10.1109/JSEN.2014.2364122

[60] Jiang, Lirong, Dakuan Yu, Hong Gao, Dongpo Xu, Bo Wang and Xueguang Qiao. "A Fiber Bragg Grating accelerometer with cantilever beam." *Optical Fiber Technology* 74 (2022): 103088. https://doi.org/10.1016/j.yofte.2022.103088

[61] Fuhr, Peter L., Stephanus J. Spammer and Yinian Zhu. "A novel signal demodulation technique for chirped Bragg grating strain sensors." *Smart materials and structures* 9, no. 1 (2000): 85. https://doi.org/10.1088/0964-1726/9/1/309

[62] Huebner, Kenneth H., Donald L. Dewhirst, Douglas E. Smith and Ted G. Byrom. *The finite element method for engineers*. John Wiley & Sons, 2001.

[63] Basumallick, Nandini, Palas Biswas, Rajib Chakraborty, Sushanta Chakraborty, Kamal Dasgupta and Somnath Bandyopadhyay. "Fibre Bragg grating based accelerometer with extended bandwidth." *Measurement Science and Technology* 27, no. 3 (2016): 035008. https://doi.org/10.1088/0957-0233/27/3/035008

[64] Zhu, Yinian, Ping Shum, Chao Lu, B. M. Lacquet, P. L. Swart and S. J. Spammer. "Temperature-insensitive fiber Bragg grating accelerometer." *IEEE Photonics Technology Letters* 15, no. 10 (2003): 1437-1439. https://doi.org/10.1109/LPT.2003.818048

[65] Zhang, Xiaolei, Qiangzhou Rong, Hao Sun, Shen Yang, Liutong Yuan and Manli Hu. "Low-frequency fiber Bragg grating accelerometer based on a double-semicircle cantilever." *Optical Fiber Technology* 20, no. 3 (2014): 190-193. https://doi.org/10.1016/j.yofte.2014.01.006

[66] Casas-Ramos, Miguel A. and G. E. Sandoval-Romero. "Cantilever beam vibration sensor based on the axial property of fiber Bragg grating." *Smart Struct. Syst* 19 (2017): 625-631.

[67] Gere, J. M. and B. J. Goodno. "Mechanics of Materials (Cenegage Learning, 2013)." *ICAA17*.

[68] Wang, Du, Yue Wu, Yanming Song, Yongqian Wang and Lianqing Zhu. "A double-mass block acceleration sensor based on FBG." *Optical Fiber Technology* 66 (2021): 102681. https://doi.org/10.1016/j.yofte.2021.102681

[69] Qiu, Zhongchao, Rui Sun, Yuntian Teng, Ning Chen and Li Hong. "Design and test of a low frequency fiber Bragg grating acceleration sensor with double tilted cantilevers." *Optics communications* 507 (2022): 127663. https://doi.org/10.1016/j.optcom.2021.127663

[70] N. S. Khalid, M. F. Hassan and M. R. Rahim, "A modal-based approach for modelling the cantilever FBG accelerometer with the presence of tip mass and its sensitivity analysis," Optik, vol. 271, p. 170209, 2022, https://doi.org/10.1016/j.ijleo.2022.170209

[71] Khalid, Nor Syukriah, Mohd Firdaus Hassan, Mohd Hafizi Zohari and Muhammad Rais Rahim. "A strain-wavelength modelling of low-frequency cantilever fibre Bragg grating accelerometer." *Proceedings of the Institution of Mechanical Engineers, Part C: Journal of Mechanical Engineering Science* 235, no. 23 (2021): 6711-6723. https://doi.org/10.1177/09544062211008929

[72] Liu, Fufei, Yutang Dai, Joseph Muna Karanja and Minghong Yang. "A low frequency FBG accelerometer with symmetrical bended spring plates." *Sensors* 17, no. 1 (2017): 206. https://doi.org/10.3390/s17010206

[73] Wei, Li, Dazhou Jiang, Lingling Yu, Hengchun Li and Zhuang Liu. "A novel miniaturized fiber Bragg grating vibration sensor." *IEEE Sensors Journal* 19, no. 24 (2019): 11932-11940. https://doi.org/10.1109/JSEN.2019.2936596

[74] Luo, Xiaodong, Yongfang Li, Jianxin Zhang and Hong Gao. "A fiber Bragg grating accelerometer based on Y-shaped symmetrical beam structure." *Optical Fiber Technology* 66 (2021): 102649. https://doi.org/10.1016/j.yofte.2021.102649

[75] Chen, Fengyi, Xingyong Li, Ruohui Wang and Xueguang Qiao. "Sensitivity enhancement of fiber-optic accelerometers using thin-cladding fiber Bragg gratings." *Journal of Lightwave Technology* 39, no. 18 (2021): 5988-5994. https://doi.org/10.1109/JLT.2021.3091518

[76] Parida, Om Prakash, Jagannath Nayak and Sundarrajan Asokan. "Design and validation of a novel high sensitivity self-temperature compensated fiber Bragg grating accelerometer." *IEEE Sensors Journal* 19, no. 15 (2019): 6197-6204. https://doi.org/10.1109/JSEN.2019.2909186

[77] Li, Tianliang, Yuegang Tan and Zude Zhou. "A fiber Bragg grating sensing-based micro-vibration sensor and its application." *Sensors* 16, no. 4 (2016): 547. https://doi.org/10.3390/s16040547
[78] Li, Tianliang, Yuegang Tan, Zude Zhou, Li Cai and Ruiya Li. "Research on pasted FBG-based accelerometer's sensitization process method and its characteristics." *IEICE Electronics Express* 12, no. 17 (2015): 20150583-20150583. https://doi.org/10.1587/elex.12.20150583
[79] Muller, Mathias S., Thorbjorn C. Buck and Alexander W. Koch. "Fiber Bragg grating-based acceleration sensor." In *2009 International Symposium on Optomechatronic Technologies*, pp. 127-132. IEEE, 2009. https://doi.org/10.1109/ISOT.2009.5326111
[80] Li, X. C., Su Liu, W. T. Zhang, F. X. Zhang, F. Li and Y. L. Liu. "Study on low-frequency characteristic of double-diaphragm fiber Bragg grating geophone." *J. Optoelectron. Laser* 21, no. 4 (2010): 529-532.
[81] Liu, Qinpeng, Xue He, Xueguang Qiao, Tong Sun and Kenneth TV Grattan. "Design and modeling of a high sensitivity fiber Bragg grating-based accelerometer." *IEEE Sensors Journal* 19, no. 14 (2019): 5439-5445. https://doi.org/10.1109/JSEN.2019.2904218
[82] Weng, Yinyan, Xueguang Qiao, Tuan Guo, Manli Hu, Zhongyao Feng, Ruohui Wang and Jing Zhang. "A robust and compact fiber Bragg grating vibration sensor for seismic measurement." *IEEE sensors journal* 12, no. 4 (2011): 800-804. https://doi.org/10.1109/JSEN.2011.2166258
[83] Li, Kuo, Tommy HT Chan, Man Hong Yau, Theanh Nguyen, David P. Thambiratnam and Hwa Yaw Tam. "Very sensitive fiber Bragg grating accelerometer using transverse forces with an easy over-range protection and low cross axial sensitivity." *Applied Optics* 52, no. 25 (2013): 6401-6410. https://doi.org/10.1364/AO.52.006401
[84] Li, Kuo, Guoyong Liu, Yuqing Li, Jun Yang and Wenlong Ma. "Ultra-small fiber Bragg grating accelerometer." *Applied Sciences* 9, no. 13 (2019): 2707. https://doi.org/10.3390/app9132707
[85] Lee, Yeon-Gwan, Dae-Hyun Kim and Chun-Gon Kim. "Transmissive grating-reflective mirror-based fiber optic accelerometer for stable signal acquisition in industrial applications." *Optical Engineering* 51, no. 5 (2012): 054402-054402. https://doi.org/10.1117/1.OE.51.5.054402
[86] Wang, Xiaofeng, Yongxing Guo, Li Xiong and Heng Wu. "High-frequency optical fiber Bragg grating accelerometer." *IEEE Sensors journal* 18, no. 12 (2018): 4954-4960. https://doi.org/10.1109/JSEN.2018.2833885
[87] Hong, Li, Jinquan Zhang, Ruilei Zhang, Peng Wu and Li Duan. "Research on low-frequency FBG accelerometer based on double curved beam reed." *Optics Communications* 543 (2023): 129615. https://doi.org/10.1016/j.optcom.2023.129615
[88] National Instruments Corp. "Measuring Vibration with Accelerometers." https://www.ni.com/en-my/innovations/white-papers/06/measuring-vibration-with-accelerometers.html
[89] Saktioto, Toto and Jalil Ali. *Non Linear Optic in Fiber Bragg Grating*. IntechOpen, 2012. https://doi.org/10.5772/35250
[90] Xu, Wenjie, Qiang Bian, Jianqiao Liang, Zhencheng Wang, Yang Yu and Zhou Meng. "Recent advances in optical fiber high-temperature sensors and encapsulation technique." *Chinese Optics Letters* 21, no. 9 (2023): 090007. https://doi.org/10.3788/COL202321.090007
[91] Li, Hong-Nan, Guang-Dong Zhou, Liang Ren and Dong-Sheng Li. "Strain transfer analysis of embedded fiber Bragg grating sensor under nonaxial stress." *Optical Engineering* 46, no. 5 (2007): 054402-054402. https://doi.org/10.1117/1.2739554
[92] Timoshenko, S. "Vibration problems in engineering 2nd edn." (1937).
[93] Dietl, J. M., A. M. Wickenheiser and E. Garcia. "A Timoshenko beam model for cantilevered piezoelectric energy harvesters." *Smart Materials and Structures* 19, no. 5 (2010): 055018. https://doi.org/10.1088/0964-1726/19/5/055018
[94] Korayem, M. H., A. M. Shafei, F. Absalan, B. Kadkhodaei and A. Azimi. "Kinematic and dynamic modeling of viscoelastic robotic manipulators using Timoshenko beam theory: theory and experiment." *The International Journal of Advanced Manufacturing Technology* 71 (2014): 1005-1018. https://doi.org/10.1007/s00170-013-5391-1
[95] Franza andrea, Sinan Acikgoz and Matthew J. DeJong. "Timoshenko beam models for the coupled analysis of building response to tunnelling." *Tunnelling and Underground Space Technology* 96 (2020): 103160. https://doi.org/10.1016/j.tust.2019.103160
[96] Kourtis, Lampros C., Dennis R. Carter and Gary S. Beaupre. "Improving the estimate of the effective elastic modulus derived from three-point bending tests of long bones." *Annals of biomedical engineering* 42 (2014): 1773-1780. https://doi.org/10.1007/s10439-014-1027-3
[97] Sun, Zhendong, Lianzhi Yang and Yang Gao. "The displacement boundary conditions for Reddy higher-order shear cantilever beam theory." *Acta Mechanica* 226, no. 5 (2015): 1359-1367. https://doi.org/10.1007/s00707-014-1253-7

[98] Bishop, Richard Evelyn Donohue, William Geraint Price and Zhang Xi Cheng. "On the structural dynamics of a Vlasov beam." *Proceedings of the Royal Society of London. A. Mathematical and Physical Sciences* 388, no. 1794 (1983): 49-73. https://doi.org/10.1098/rspa.1983.0072

[99] Hassan, Mohd Firdaus, Nor Syukriah Khalid and M. R. Rahim. "Sensitivity identification of low-frequency cantilever fibre Bragg grating accelerometer using cascade-forward backpropagation neural network." *International Journal of Automotive and Mechanical Engineering* 19, no. 1 (2022): 9419-9432. https://doi.org/10.15282/ijame.19.1.2022.06.0725

[100] Khalid, Nor Syukriah and Mohd Firdaus Hassan. "Sensitivity identification of low-frequency cantilever fibre Bragg grating accelerometer." *International Journal of Integrated Engineering* 13, no. 7 (2021): 235-244. https://doi.org/10.30880/ijie.2021.13.07.027